

Nematic liquid crystals as a new challenge for radiative transfer[†]

Bart van Tiggelen

Laboratoire de Physique et Modélisation des Systèmes Complexes/ CNRS, Maison des
Magistères, Université Joseph Fourier, B.P. 166, F-38042 Grenoble Cedex 9,
France

Holger Stark

Institut für Theoretische und Angewandte Physik, Universität Stuttgart, Pfaffenwaldring 57,
D-70550 Stuttgart, Germany

Radiative transfer has been studied for almost a century, but only recently have effects of broken symmetry in the diffusion of light been systematically studied. Familiar concepts such as the mean free path and the diffusion constant must be generalized. Nematic liquid crystals provide a realistic complex system in which the new concepts are relevant. Thermal fluctuations of the local optical axis generate a weak but very specific and anisotropic light scattering and can even be long range. In addition, two different modes of electromagnetic propagation exist, with different polarization, and with different speeds, that couple in multiple scattering. It becomes a challenge to describe optical phenomena such as birefringence, interference, polarization, and intensity fluctuations under such conditions. In this review, the authors first describe the interesting phenomena in radiative transfer in complex anisotropic media and nematic liquid crystals. They then develop the systematic theory of transport starting from the fundamental equations and going through a Green's-function formulation.

CONTENTS

I. Radiative Transfer: An Old Subject, but Still Very Much Alive	1017
II. Nematic Liquid Crystals: What We Have Known for a Long Time	1019
A. Optics of homogeneous nematic liquid crystals	1019
B. Thermal fluctuations of the nematic director	1021
C. Single light scattering from director fluctuations	1022
III. Light Diffusion and Hidden Consequences of Rotational Symmetry	1023
IV. Anisotropic Light Diffusion in Nematics	1026
A. "Back-of-the-envelope" calculations	1026
1. Equipartition of polarization in the diffuse regime	1027
2. Dynamic correlations	1027
B. Rigorous transport theory	1028
1. Reciprocity and flux conservation	1029
2. Dyson's equation in nematics	1029
3. Bethe-Salpeter equation in nematics	1030
4. Qualitative discussions	1033
C. Diffuse transmission from a nematic cell	1035
V. Conclusions and Future Prospects	1036
Acknowledgments	1037
References	1038

*Met Uw toverstok kunt U niets bezweren,
Eerst moet Gij de formules leren.*¹

I. RADIATIVE TRANSFER: AN OLD SUBJECT, BUT STILL VERY MUCH ALIVE

Since its introduction at the beginning of this century, the study of radiative transfer has attracted continuous

interest in physics. The starting point was the equation of radiative transfer (Schuster, 1905), which is a phenomenological bookkeeping method for keeping track of scattered and absorbed light in a heterogeneous medium.

The mathematical complexity of this equation has given rise to many detailed numerical and analytical studies, mostly initiated by astrophysicists in an effort to understand multiple light scattering in stellar atmospheres and interstellar clouds (Chandrasekhar, 1960; Sobolev, 1963; Sobolev, 1975; Mihalas, 1978; van de Hulst, 1980). Even the simplest problem in radiative transfer, the classical Milne problem, describing stationary scattering of scalar waves from isotropic point scatterers in a semi-infinite medium, still serves as a numerical practice problem for students. Sophisticated numerical codes, each claimed to be better than the last, can be found on the Internet for a wide variety of applications and boundary conditions. Since the beginning of the 1980s, research has begun to focus on physics "beyond classical radiative transfer," with emphasis on two aspects: mesoscopic physics and complex media.

The first basic question is how radiative transfer—a macroscopic transport phenomenon—is compatible with the underlying Maxwell equations, which should in principle provide a complete description. Classical radiative transfer suffers from two limitations. First, it ignores the wave nature of light. Second, in phenomenological radiative transfer, an average is performed implicitly. As a result it deals with the mean flow of energy only, and does not include any (temporal) fluctuations. These limitations have led to more microscopic studies of radiative transfer, which have acquired their own name: *mesoscopics*. They aim to describe a regime between the microscopic world of wave equations and the macroscopic world of transport equations.

[†]This work is dedicated to Professor Dr. Hendrik Christoffel van de Hulst, pioneer in light scattering, who died in Leiden (the Netherlands) on 31 July 2000 at the age of 81.

¹Dutch saying expressing the idea that exact science relies on mathematics and not on magic.

Mesoscopic studies have led to many significant discoveries. Most of them originally concentrated on electron waves in condensed matter (Akkermans *et al.*, 1995), but it was soon realized that most new developments have counterparts in classical waves physics (John, 1991; van Rossum and Nieuwenhuizen, 1999). The first phenomenon “beyond” conventional radiative transfer, discovered in 1985 and now called coherent backscattering (Kuga and Ishimaru, 1984; van Albada and Lagendijk, 1985; Wolf and Maret, 1985; Akkermans, Wolf, and Maynard, 1986), is an interference effect that survives in multiple scattering. Since its discovery, many aspects of this phenomenon have been studied in great detail (van Tiggelen and Maynard, 1997; POAN Research Group, 1998). Fluctuations in light transmission have been investigated, leading to the discovery of long-range correlations (de Boer *et al.*, 1990; Genack, 1990; Genack and Garcia, 1993; Scheffold and Maret, 1998). Although experiments deal with samples much bigger than the mean free path, i.e., they are macroscopic, the description of long-range intensity fluctuations requires a rigorous treatment of wave behavior at the microscopic level (Berkovits and Feng, 1994; Sheng, 1995; van Rossum and Nieuwenhuizen, 1999), thereby introducing a completely new “mesoscopic” regime of radiative transfer.

Radiative transport in complex systems has also been subject to intense study in recent years. Common complex materials under discussion range from liquid crystals, foams (Durian, Weitz, and Pine, 1991; Höhler, Cohen-Addad, and Hoballah, 1997), emulsions (Gang, Krall, and Weitz, 1994), and magneto-rheological fluids (Furst and Gast, 1998), to cirrus clouds (Mishchenko, Travis, and Hovenier, 1999), actin networks (Gisler and Weitz, 1999), and human tissue. In “complex” situations, the best phenomenological treatment of radiative transfer is not always obvious. Different communities have focused on different aspects of the subject. Astrophysicists and scientists interested in remote sensing are now studying the scattering of light and radiation from nonspherical particles (Mishchenko, Travis, and Hovenier, 1999). Scientists more oriented towards condensed matter study media with extreme disorder, i.e., media with high optical contrast and a high packing fraction, such as semiconductor powders. A recent experiment (Wiersma *et al.*, 1997) claims localization of infrared light in powders of GaAs. Wave localization, which is expected to happen when the mean free path becomes as small as the wavelength, refers to a complete halt of radiative transfer due to destructive interferences. It was put forward by condensed-matter physicists some 40 years ago to explain disorder-driven metal-insulator transitions, and has been subject to wide attention in physics and mathematics (van Tiggelen, 1999). Soft-matter physicists use radiative transfer to investigate the dynamics of turbid media with the method called diffusing wave spectroscopy (Maret, 1997). In this method one studies the temporal correlation function of light intensity in the multiple-scattering regime and generalizes the

well-known technique of quasielastic light scattering that has been widely applied in the single-scattering regime.

The complex nature of wave transport can arise from an unconventional environment or from unconventional constraints. Complex media in particular are now subject to many interdisciplinary collaborations, since the applications using these media are both numerous and wide-ranging. Studies of multiple scattering of elastic waves in the Earth’s crust are now being undertaken to understand the long-time codas that are observed after earthquakes (Campillo, Margerin, and Shapiro, 1999). Light propagation in human tissue (Chance, 1989; Boas, Campbell, and Yodh, 1995; Yodh and Chance, 1995; Virmont and Ledanois, 1998) is characterized by special geometry, inhomogeneous scattering and absorption, and time dependence, and many efforts are being made to take advantage of radiative transfer theory to image in a reliable and realistic way (Boas *et al.*, 1994; Heckmeier *et al.*, 1997). Atomic gases are another example of a popular complex medium for multiple light scattering. Although this medium was originally studied from the starting point of the radiative transport equation (Holstein, 1947), recent developments in atom cooling have made possible interference studies in cold gases (Labeyrie *et al.*, 1999).

Some complex media are characterized by a broken continuous symmetry that transforms an originally simple problem rapidly into an intractable set of complicated equations. Intuitive steps become less evident, since phenomenological descriptions implicitly assume a variety of symmetries. Rotational symmetry, for example, requires that—on average—all directions in space be equivalent. A nonspherical particle induces a local anisotropy, but averaging over all its directions restores global rotational symmetry. A nematic liquid crystal is an example of a complex system that scatters light and in which rotational symmetry of the isotropic liquid is broken. Another contemporary example occurs in the magneto-optics of diffuse light (Rikken and van Tiggelen, 1996), where the presence of an external homogeneous magnetic field breaks rotational symmetry.

A magnetic field also breaks time-reversal symmetry in light propagation and is, for that reason, an important tool for controlling symmetry in radiative transfer. Time-reversal symmetry is broken by the (often implicitly adopted) ensemble averaging in the equation of radiative transfer. It is possible to influence interference effects in multiple light scattering with a magnetic field (Erbacher, Lenke, and Maret, 1993), as was seen with mesoscopic electron waves (Sharvin and Sharvin, 1981). Similar time-reversal studies with acoustic waves—the magnetic field being replaced by liquid vortices—have been carried out by Roux and Fink (1995). Both this study and that of Sharvin and Sharvin have shown the considerable sensitivity sensibility of multiple scattering of waves to broken time reversal, a conclusion that is confirmed by recent developments in random-matrix theory (Beenakker, 1997). In addition, acoustic studies have established a robust time reversal in high-order

multiple scattering (Derode, Roux, and Fink, 1995), which is not expected for classical particles. Multiple scattering of light has recently been investigated in chiral media, where mirror symmetry is broken. Since sugar is chiral, such studies may be relevant to medical imaging (Silverman *et al.*, 1999).

In keeping with the larger goal of understanding radiative transfer in systems with broken symmetries. The aim of the present work is to introduce the reader to an approach that links Maxwell's equations to the equations of radiative transfer, going through all the important steps in a self-contained way. This is necessary in order to understand the consequences of broken symmetry in multiple light scattering. In this review we shall focus on nematic liquid crystals as a concrete example. This choice is motivated by experiments that have been carried out on coherent backscattering of light in multidomain nematic liquid crystals (Vlasov *et al.*, 1988) and monodomain liquid crystals (Vithana, Asfaw, and Johnson, 1993), as well as static and dynamic measurements of diffusing light (Kao *et al.*, 1997; Wiersma *et al.*, 1999) in aligned nematics. We hope that our approach may serve as a more general guide to the formulation multiple waves scattering in complex media.

The review is organized as follows. In Sec. II we introduce nematic liquid crystals as a medium for optics and discuss the optical properties that affect light scattering in nematic liquid crystals. In Sec. III we introduce a common and popular simplification in radiative transfer—the diffusion approximation—to describe the multiple scattering of light. This approximation avoids the complex equation of radiative transport. We introduce basic concepts and outline their consequences in “simple” media. Finally, in Sec. IV, we treat multiple scattering in nematic liquid crystals and concentrate on properties that make multiply scattered light in these systems unusual and unfamiliar, such as anisotropic diffuse transport and polarization of diffuse light.

II. NEMATIC LIQUID CRYSTALS: WHAT WE HAVE KNOWN FOR A LONG TIME

The nematic liquid-crystalline phase consists of rod-like organic molecules that tend to align parallel to each other but that show no long-range positional order of their centers of mass. The local average direction of the molecules is described by a unit vector $\mathbf{n}(\mathbf{r}, t)$ called the Frank director. It gives the direction of the optical axis and appears in the local dielectric tensor

$$\varepsilon_{ij}(\mathbf{r}, t) = \varepsilon_{\perp} \delta_{ij} + \varepsilon_a n_i(\mathbf{r}, t) n_j(\mathbf{r}, t), \quad (1)$$

where ε_{\perp} and $\varepsilon_{\parallel} = \varepsilon_a + \varepsilon_{\perp}$ are the dielectric constants for electric fields, perpendicular and parallel respectively, to the director, and where $\varepsilon_a = \varepsilon_{\parallel} - \varepsilon_{\perp}$ stands for the dielectric anisotropy. In the nematic state, the dielectric anisotropy is proportional to the Maier-Saupe order parameter S , $\varepsilon_a \propto S$, which characterizes how well the molecules are aligned along the local director \mathbf{n} . In a mean-field approach $S \propto (T^{\dagger} - T)^{1/2}$, where T^{\dagger} is a temperature slightly above the nematic-isotropic transition

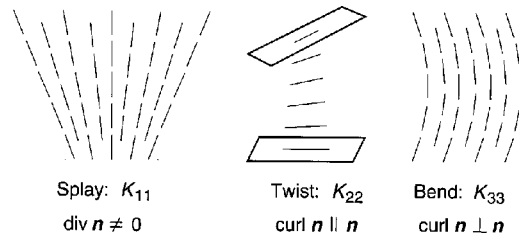


FIG. 1. Pure splay, twist, and bend deformations for nematic liquid crystals.

temperature T_c , indicating a weak first-order phase transition. Since the liquid-crystal molecules very often carry a permanent electric dipole moment, the frequency dependence of the dielectric constants follows Debye's classical relaxation theory, with values of the order of 10. Typical relaxation frequencies are around 100 MHz for ε_{\perp} and 1–10 MHz for ε_{\parallel} (de Jeu, 1980; Vertogen and de Jeu, 1988). At optical frequencies, the dielectric constants are determined only by the molecular electronic polarizability and are typically equal to 2.5–3.

The energetically favored state of a nematic phase is a uniform director field $\mathbf{n}(\mathbf{r}, t) = \mathbf{n}_0$ throughout the sample. Its distortion costs energy, which can be calculated from the Oseen-Zöcher-Frank free energy (De Gennes and Prost, 1993; Chaikin and Lubensky, 1995):

$$F[\mathbf{n}] = \frac{1}{2} \int d^3r [K_1(\nabla \cdot \mathbf{n})^2 + K_2(\mathbf{n} \cdot \nabla \times \mathbf{n})^2 + K_3(\mathbf{n} \times \nabla \times \mathbf{n})^2 - \Delta\chi(\mathbf{n} \cdot \mathbf{H})^2], \quad (2)$$

where K_1 , K_2 , and K_3 are the Frank elastic constants describing, respectively, the free energy associated with splay, twist, and bend distortions (see Fig. 1). We also include a magnetic-field term with $\Delta\chi = \chi_{\parallel} - \chi_{\perp}$ the anisotropy of the magnetic susceptibility. If $\Delta\chi > 0$, an alignment of the director parallel to the field \mathbf{H} will be favored. In Eq. (2) we did not include any surface contributions to the free energy. In particular, the saddle-splay (K_{24}) and the splay-bend (K_{13}) terms have been omitted (Nehring and Saupe, 1971; Pergamenschik, 1998). Their optical consequences have been investigated by Shalaginov (1994).

Even in a uniformly aligned sample, thermally induced fluctuations of the director exist:

$$\mathbf{n}(\mathbf{r}, t) = \mathbf{n}_0 + \delta\mathbf{n}(\mathbf{r}, t). \quad (3)$$

They lead to fluctuations in the local dielectric tensor that scatter light. This is the physical process for which we want to formulate the theory of multiple light scattering. To do so, we first have to look at light propagation in a homogeneous uniaxial medium (Sec. II.A). In Sec. II.B we consider fluctuations of the director, and finally Sec. II.C introduces the structure factor that will describe single-light-scattering events.

A. Optics of homogeneous nematic liquid crystals

A nematic liquid crystal is, on average, a homogeneous uniaxial medium and therefore birefringent for

light traveling inside. Light propagates through such a system in two characteristic modes. The ordinary light ray behaves as in an isotropic system. However, the extraordinary light mode possesses a direction-dependent index of refraction, its phase and group velocities are not equal to each other, and the electric-field vector is not transverse. In the following, we review these facts, look at the energy density and the Poynting vector, and introduce some notation for further use. Our review contains details, since they are important for the understanding of radiative transfer in uniaxial systems. It may also serve as a collection of formulas for people interested in such systems.

In general, Maxwell's equations are coupled to the hydrodynamic equations of the liquid crystal in a complicated way (Liu, 1994). We simplify by considering the liquid crystal as a macroscopic, local and instantaneous, linear but anisotropic dielectric medium, as described by the constitutive equations

$$D_i(\mathbf{r},t) = \varepsilon_{ij}(\mathbf{r},t)E_j(\mathbf{r},t) \quad \text{and} \quad B_i(\mathbf{r},t) = H_i(\mathbf{r},t), \quad (4)$$

where \mathbf{B} and \mathbf{H} are, respectively, the magnetic induction and magnetic field. The time dependence in this equation refers to slow (microsecond) temporal variations of the director and not to the fast (femtosecond) cycles of the electromagnetic field. The magnetic permeability is close to unity in liquid crystals, and its effect can be totally neglected compared to the induced polarization described by the dielectric tensor. Light propagation is then determined by the Helmholtz wave equation for the electric light field $\mathbf{E}(\mathbf{r},t)$:

$$\left[-\nabla^2 \delta_{ij} + \nabla_i \nabla_j + \frac{1}{c_0^2} \frac{\partial^2}{\partial t^2} \varepsilon_{ij}(\mathbf{r},t) \right] E_j(\mathbf{r},t) = 0. \quad (5)$$

To discuss light propagation in a homogeneous nematic, we shall first ignore fluctuations of the dielectric tensor and adopt Eq. (1) with the equilibrium Frank director \mathbf{n}_0 leading to a constant dielectric tensor ε_0 . In that case the stationary solutions for the electric field are plane waves $\mathbf{E} = \mathbf{e}_\alpha \exp(i\mathbf{k}_\alpha \cdot \mathbf{r}) \exp(-i\omega t)$, with wave vector $\mathbf{k}_\alpha = k_\alpha \hat{\mathbf{k}}$, frequency ω , and a polarization vector $\mathbf{e}_\alpha(\hat{\mathbf{k}})$ that obeys a generalized eigenvalue equation (Lax and Nelson, 1971; Landau, Lifshitz, and Pitaevskii, 1984, Sec. 98; Boots, 1994; Stark and Lubensky, 1997):

$$\left[\mathbf{1} - \hat{\mathbf{k}} \otimes \hat{\mathbf{k}} - \frac{1}{n_\alpha(\hat{\mathbf{k}})^2} \varepsilon_0 \right] \mathbf{e}_\alpha(\hat{\mathbf{k}}) = 0. \quad (6)$$

For future use we have defined $\mathbf{a} \otimes \mathbf{b}$ as a second-rank tensor with components $a_i b_j$. In Eq. (6) we introduced the direction-dependent index of refraction $n_\alpha(\hat{\mathbf{k}}) \equiv c_0 k_\alpha / \omega$. It is to be determined for the three possible electric-field modes, to be referred to as ordinary ($\alpha = o$), extraordinary ($\alpha = e$), and longitudinal ($\alpha = l$). The third solution corresponds to a nonpropagating mode with $n_l = \infty$ and $\mathbf{e}_l(\hat{\mathbf{k}})$ parallel to the wave vector \mathbf{k}_l and will hardly be important for scattering at optical frequencies. It is sometimes convenient to normalize the vectors $\mathbf{e}_\alpha(\hat{\mathbf{k}})$ such that the associated energy density

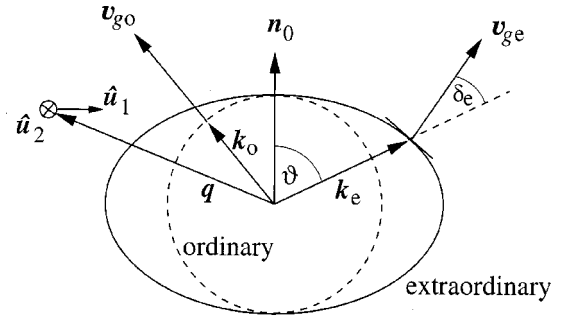


FIG. 2. Constant frequency surface for ordinary and extraordinary light rays, seen in the plane spanned by the optical axis (\mathbf{n}_0) and the wave vector. The ordinary light ray has a constant index of refraction $\sqrt{\varepsilon_\perp}$. The wave vector \mathbf{k}_o and the group velocity \mathbf{v}_{g_o} are parallel to each other. The extraordinary wave has an ellipsoidal index of refraction that equals $\sqrt{\varepsilon_\perp}$ only along the optical axis; \mathbf{k}_e and \mathbf{v}_{g_e} enclose an angle δ_e . The figure corresponds to a positive dielectric anisotropy ($\varepsilon_a > 0$) so that the extraordinary ellipsoid is located outside the ordinary sphere. In diffusing light, ordinary waves therefore have the minority (see Sec. IV.A.1). The two vectors $\hat{\mathbf{u}}_1$ and $\hat{\mathbf{u}}_2$, characterize the two director modes of wave vector \mathbf{q} .

$(\mathbf{E} \cdot \varepsilon_0 \mathbf{E} + \mathbf{H} \cdot \mathbf{H})/8\pi$, averaged over one cycle, is normalized to one. This requires that $\mathbf{e}_\alpha \cdot \varepsilon_0 \mathbf{e}_\alpha = 1$ (Stark and Lubensky, 1997). We shall use this convention. However, at several places in this work it turns out to be handy to normalize the polarization vectors to $|\mathbf{e}_\alpha| = 1$. We shall denote these cases by $\hat{\mathbf{e}}_\alpha$.

The ordinary solution to the eigenvalue (6), a pure transverse wave, can be readily checked with the help of Eq. (1). It possesses an index of refraction, $n_o = \sqrt{\varepsilon_\perp}$, and a polarization vector $\mathbf{e}_o(\hat{\mathbf{k}}) = \hat{\mathbf{u}}_2/n_o$, and it is perpendicular to both the Frank director \mathbf{n}_0 and the wave vector \mathbf{k}_o , enclosing the angle ϑ (see Fig. 2). The second solution, for an extraordinary light ray, has its polarization vectors in the plane spanned by \mathbf{n}_0 and \mathbf{k}_e :

$$\mathbf{e}_e(\hat{\mathbf{k}}) = n_e(\hat{\mathbf{k}}) \left[-\frac{\sin \vartheta}{\varepsilon_\parallel} \mathbf{n}_0 + \frac{\cos \vartheta}{\varepsilon_\perp} \hat{\mathbf{u}}_1(\hat{\mathbf{k}}) \right], \quad (7)$$

where we used the unit vector $\hat{\mathbf{u}}_1(\hat{\mathbf{k}}) \equiv \mathbf{n}_0 \times \hat{\mathbf{u}}_2(\hat{\mathbf{k}})$ perpendicular to \mathbf{n}_0 . We notice that generally $\mathbf{e}_e(\hat{\mathbf{k}})$ possesses a longitudinal component. The refractive index $n_e(\hat{\mathbf{k}})$ is given by the relation

$$\frac{1}{n_e^2(\hat{\mathbf{k}})} = \frac{\sin^2 \vartheta}{\varepsilon_\parallel} + \frac{\cos^2 \vartheta}{\varepsilon_\perp}. \quad (8)$$

The phase velocity for wave propagation in homogeneous media is given by $\mathbf{v}_{p\alpha} = \hat{\mathbf{k}} c_0 / n_\alpha$. However, in anisotropic systems there also exists a group velocity that, in contrast to isotropic systems, has to be distinguished carefully from the phase velocity. Let us consider this difference in more detail. Light modes are characterized by a dispersion relation $\omega(\mathbf{k}_\alpha) = c_0 k_\alpha / n_\alpha$ for each polarization α , which, at a given frequency ω , determines the wave vector $\mathbf{k}_\alpha \equiv n_\alpha \omega \hat{\mathbf{k}} / c_0$. In the case of an extraordinary ray, the wave number k_e depends on the direction

TABLE I. Material parameters (Stephen and Straley, 1974; Collings, 1997) for three typical liquid crystals: 5CB, PAA, and MBBA at temperature T .

	T [K]	ε_{\perp}	ε_a	$\Delta\chi$	K_1 [dyne]	K_2 [dyne]	K_3 [dyne]	γ [cps]
5CB	303	2.38	0.54	0.96×10^{-7}	4.2×10^{-7}	2.3×10^{-7}	5.3×10^{-7}	81.0
PAA	398	2.45	0.90	1.18×10^{-7}	4.5×10^{-7}	2.9×10^{-7}	9.5×10^{-7}	5.8
MBBA	298	2.37	0.69	0.97×10^{-7}	6×10^{-7}	4×10^{-7}	7.5×10^{-7}	77

of propagation. For a given frequency ω , the wave vector \mathbf{k}_{α} lies on the *constant-frequency surface*, which is a circle of radius $\sqrt{\varepsilon_{\perp}}\omega/c_0$ for the ordinary ray ($\alpha=o$) and, as shown in Fig. 2, an ellipse with semiaxes $\sqrt{\varepsilon_{\perp}}\omega/c_0$ and $\sqrt{\varepsilon_{\parallel}}\omega/c_0$ for an extraordinary light wave. For each polarization, electromagnetic energy is transported along the direction of the group velocity defined by

$$\mathbf{v}_{g\alpha} = \nabla_{\mathbf{k}} \omega_{\alpha}(\mathbf{k}), \quad (9)$$

hence $\mathbf{v}_{g\alpha}$ is normal to the constant-frequency surface. For an ordinary ray, the phase and group velocity are both equal to $\hat{\mathbf{k}}c_0/n_o$. However, the group velocity of an extraordinary wave,

$$\mathbf{v}_{ge} = c_0 n_e(\hat{\mathbf{k}}) \left(\frac{\cos \vartheta}{\varepsilon_{\perp}} \mathbf{n}_0 + \frac{\sin \vartheta}{\varepsilon_{\parallel}} \hat{\mathbf{u}}_1 \right), \quad (10)$$

generally encloses a nonzero angle δ_e with the phase velocity, as illustrated in Fig. 2. This angle is given by

$$\cos \delta_e = \frac{1}{n_e^2(\hat{\mathbf{k}})} \left(\frac{\sin^2 \vartheta}{\varepsilon_{\parallel}^2} + \frac{\cos^2 \vartheta}{\varepsilon_{\perp}^2} \right)^{-1/2}. \quad (11)$$

The angle δ_e is also spanned by the electric field \mathbf{E} and the displacement vector \mathbf{D} . Furthermore, it can easily be checked that the norm of the polarization vectors \mathbf{e}_{α} equals $|\mathbf{e}_{\alpha}| = |\mathbf{v}_{g\alpha}|/c_0$.

In a homogeneous medium without absorption, the Poynting vector and the group velocity must necessarily be parallel (Landau, Lifshitz, and Pitaevskii, 1984, Sec. 101, problem 1). Hence the Poynting vector $c_0(\mathbf{E} \times \mathbf{H})/4\pi$ gives the direction of energy transport. For a polarized plane wave the cycle-averaged Poynting vector equals the group velocity times the cycle-averaged energy density W^{α} : $\mathbf{S}^{\alpha} = W^{\alpha} \mathbf{v}_{g\alpha}$.

B. Thermal fluctuations of the nematic director

Since we are dealing with finite temperatures, the director will fluctuate around its equilibrium value, so that $\mathbf{n}(\mathbf{r}, t) = \mathbf{n}_0 + \delta\mathbf{n}(\mathbf{r}, t)$. For small fluctuations we must have $\delta\mathbf{n}(\mathbf{r}, t) \perp \mathbf{n}_0$ since $\mathbf{n}(\mathbf{r}, t)$ is a unit vector. Let $\delta\mathbf{n}(\mathbf{q}, t)$ be the Fourier transform of $\delta\mathbf{n}(\mathbf{r}, t)$. It is customary to express $\delta\mathbf{n}(\mathbf{q}, t)$ in the basis shown in Fig. 2,

$$\delta\mathbf{n}(\mathbf{q}, t) = \delta n_1(\mathbf{q}, t) \hat{\mathbf{u}}_1 + \delta n_2(\mathbf{q}, t) \hat{\mathbf{u}}_2, \quad (12)$$

where the amplitudes $\delta n_{\delta}(\mathbf{q}, t)$, for $\delta=1,2$, characterize the two possible orthogonal director modes for a given direction $\hat{\mathbf{q}}$. In Fig. 2 the vector $\hat{\mathbf{u}}_1$ is parallel to the long axis of the extraordinary mode and the vector $\hat{\mathbf{u}}_2$ is per-

pendicular to both n_0 and $\hat{\mathbf{u}}_1$. Accordingly, the Frank free energy given by Eq. (2) takes the form

$$F[\mathbf{n}(\mathbf{r}, 0)] = \frac{1}{2} \sum_{\delta=1}^2 \int \frac{d^3\mathbf{q}}{(2\pi)^3} K_{\delta}(\mathbf{q}) |\delta n_{\delta}(\mathbf{q}, 0)|^2 \quad (13)$$

with ‘‘elastic constants’’

$$K_{\delta}(\mathbf{q}) = K_{\delta}[\mathbf{q}^2 - (\mathbf{q} \cdot \mathbf{n}_0)^2] + K_3(\mathbf{q} \cdot \mathbf{n}_0)^2 + \Delta\chi H^2. \quad (14)$$

For \mathbf{q} perpendicular to \mathbf{n}_0 , the director modes are either splay ($\delta=1$) or twist ($\delta=2$) modes. When \mathbf{q} is parallel to \mathbf{n}_0 , one has two degenerate bend modes. The distortions corresponding to these modes are illustrated in Fig. 1. For a general wave vector \mathbf{q} , the modes contain a combination of bend and either splay or twist deformations. In Table I we list typical values of the Frank elastic constants for the three calamitic compounds MBBA, PAA, and 5CB often used for optical experiments. Their temperature behavior follows the square of the Maier-Saupe order parameter, $K_i \propto S^2$ (de Gennes and Prost, 1993).

Quasielastic light-scattering experiments in nematics (Orsay Liquid Crystal Group, 1969) measure the time-dependent director autocorrelation function (Chandrasekhar, 1977; de Gennes and Prost, 1993)

$$\langle \delta n_{\delta}(\mathbf{q}, t) \delta n_{\delta}^*(\mathbf{q}, 0) \rangle = \frac{k_B T}{K_{\delta}(\mathbf{q})} \exp\left[-\frac{K_{\delta}(\mathbf{q})}{\eta_{\delta}(\mathbf{q})} t\right]. \quad (15)$$

The first factor in this expression results from the application of the equipartition theorem,² stating that each director mode must have an average thermal energy $k_B T/2$. The second factor reflects the hydrodynamic temporal decay of the director modes. The relaxation rate is given by the ratio of elastic— $K_{\delta}(\mathbf{q})$ —and viscous— $\eta_{\delta}(\mathbf{q})$ —forces. To arrive at this result, one has to analyze the Leslie-Erickson equations (Forster *et al.*, 1971; Chandrasekhar, 1977; de Gennes and Prost, 1993). They comprise the Navier-Stokes equations for the fluid motion of a uniaxial medium and dynamical equations for the director. The viscosity $\eta_{\delta}(\mathbf{q}) = \gamma - \mu(\mathbf{q})$ is a combination of several Leslie viscosities that appear in these equations. The most important contribution to $\eta_{\delta}(\mathbf{q})$ comes from the rotational viscosity γ , which quantifies the viscous forces hindering the rotation of the director. Typical values are listed in Table I. For wave numbers

²Because we use a continuum of \mathbf{q} vectors the equipartition theorem gives $\langle \delta n_{\delta}(\mathbf{q}, 0) \delta n_{\delta}^*(\mathbf{q}', 0) \rangle = [k_B T / K_{\delta}(\mathbf{q})] \delta(\mathbf{q} - \mathbf{q}')$. Then we set $\langle \delta n_{\delta}(\mathbf{q}, 0) \delta n_{\delta}^*(\mathbf{q}, 0) \rangle \equiv \int d^3 q' / (2\pi)^3 \langle \delta n_{\delta}(\mathbf{q}, 0) \delta n_{\delta}^*(\mathbf{q}', 0) \rangle$.

$q = 10^5 \text{ cm}^{-1}$ of visible light, the relaxation times $\tau_c = \gamma/Kq^2$ typically vary from 1 to 10 μs . Since both γ and K_i scale as S^2 (de Gennes and Prost, 1993), the relaxation times are nearly temperature independent. The term $\mu(\mathbf{q})$ contains further viscosities that not only govern the viscous flow of the fluid but also couple the flow to the director motion. In Eq. (15) we have neglected a second fast mode, whose character is predominantly that of velocity diffusion familiar from isotropic fluids. Its characteristic frequency $(\eta/\rho)q^2$ (where $\rho \approx 1 \text{ g/cm}^3$ is the mass density) is much greater than $(K/\gamma)q^2$ since $\eta/\rho \sim 10^{-1} \text{ cm}^2/\text{sec}$ largely exceeds $K/\gamma \sim 10^{-5} - 10^{-6} \text{ cm}^2/\text{sec}$.

The spatial autocorrelation functions $\langle \delta n_\delta(\mathbf{R}, 0) \delta n_\delta(\mathbf{0}, 0) \rangle$ of the two components perpendicular to the equilibrium director \mathbf{n}_0 , follow from Eq. (15) after a Fourier transformation. In the one-constant approximation ($K_1 = K_2 = K_3 \equiv K$) it reads

$$\langle \delta n_\delta(\mathbf{R}, 0) \delta n_\delta(\mathbf{0}, 0) \rangle = \frac{\varepsilon_a^2 \Lambda}{4\pi R} e^{-R/\xi}, \quad (16)$$

where the magnetic coherence length

$$\xi = \sqrt{\frac{K}{\Delta\chi H^2}} \quad (17)$$

gives the length scale over which director fluctuations are correlated. For typical magnetic fields of 1 T and $\Delta\chi = 10^{-7}$ (in SI units, 1 Pa/T^2) we obtain a coherence length of 1–3 μm . The length $\Lambda = k_B T/K$ is of the order of the molecular dimension $a \approx 1 \text{ nm}$ (de Gennes and Prost, 1993). Thus, at micron length scales where light scattering takes place, thermal correlations seem to be “weak,” although their long-range nature may turn out to be otherwise. Note that Eq. (16) is valid on length scales much larger than the molecular dimension $a \approx \Lambda \approx 1 \text{ nm}$.

C. Single light scattering from director fluctuations

Director fluctuations induce fluctuations $\delta\boldsymbol{\varepsilon}(\mathbf{r}, t)$ of the dielectric tensor, which follow from Eq. (1) to first order in $\delta\mathbf{n}(\mathbf{r}, t)$:

$$\delta\boldsymbol{\varepsilon}(\mathbf{r}, t) = \varepsilon_a [\delta\mathbf{n}(\mathbf{r}, t) \otimes \mathbf{n}_0 + \mathbf{n}_0 \otimes \delta\mathbf{n}(\mathbf{r}, t)]. \quad (18)$$

In the following we consider a scattering event in which an incoming electric-field mode with polarization α , electric polarization vector $\mathbf{e}_\alpha(\hat{\mathbf{k}}_{\text{in}})$, and wave vector $\mathbf{k}_{\text{in}}^\alpha = \omega n_\alpha \hat{\mathbf{k}}_{\text{in}}/c_0$ is scattered from one single thermal fluctuation into a scattering channel with polarization β , polarization vector $\mathbf{e}_\beta(\hat{\mathbf{k}}_{\text{out}})$, and wave vector $\mathbf{k}_{\text{out}}^\beta = \omega n_\beta \hat{\mathbf{k}}_{\text{out}}/c_0$. The weakness of the thermal fluctuations seems to guarantee the validity of the Born approximation for the scattered field. In that case the scattered electric field is proportional to the Fourier component of $\delta\boldsymbol{\varepsilon}(\mathbf{r}, t)$ projected on the initial and final polarization,

$$\delta\varepsilon_{\alpha\beta}(\mathbf{q}, t) = \mathbf{e}_\beta(\hat{\mathbf{k}}_{\text{out}}) \cdot \delta\boldsymbol{\varepsilon}(\mathbf{q}, t) \cdot \mathbf{e}_\alpha(\hat{\mathbf{k}}_{\text{in}}), \quad (19)$$

where $\mathbf{q} = \mathbf{k}_{\text{out}} - \mathbf{k}_{\text{in}}$ denotes the scattering vector. The normalization of the polarization vectors $\mathbf{e}_\alpha(\hat{\mathbf{k}})$ has been chosen such that they correspond to unit energy density, as was discussed in Sec. I.A. In (quasi)elastic experiments one probes the (temporal) autocorrelation function of the scattered electric field. In single scattering this autocorrelation function is proportional to the matrix element

$$B(\alpha \hat{\mathbf{k}}_{\text{in}} \rightarrow \beta \hat{\mathbf{k}}_{\text{out}}, t) = \frac{\omega^4}{c_0^4} \langle \delta\varepsilon_{\alpha\beta}(\mathbf{q}_s, t) \delta\varepsilon_{\alpha\beta}^*(\mathbf{q}_s, 0) \rangle. \quad (20)$$

We call $B(\alpha \hat{\mathbf{k}}_{\text{in}} \rightarrow \beta \hat{\mathbf{k}}_{\text{out}}, t)$ the dynamic structure factor because it contains information about both elastic and dynamic properties of the director modes. Using $\delta\boldsymbol{\varepsilon}(\mathbf{r}, t)$ from Eq. (18) and the director autocorrelation function of Eq. (15), we obtain

$$B(\alpha \hat{\mathbf{k}}_{\text{in}} \rightarrow \beta \hat{\mathbf{k}}_{\text{out}}, t) = \varepsilon_a^2 k_B T \frac{\omega^4}{c_0^4} \sum_{\delta=1}^2 \frac{N(\alpha, \beta, \delta)}{K_\delta(\mathbf{q}_s)} \times \exp\left[-\frac{K_\delta(\mathbf{q}_s)}{\eta_\delta(\mathbf{q}_s)} t\right] \quad (21)$$

with a geometry factor

$$N(\alpha, \beta, \delta) = [(\mathbf{n}_0 \cdot \mathbf{e}_\beta)(\hat{\mathbf{u}}_\delta \cdot \mathbf{e}_\alpha) + (\hat{\mathbf{u}}_\delta \cdot \mathbf{e}_\beta)(\mathbf{n}_0 \cdot \mathbf{e}_\alpha)]^2. \quad (22)$$

From the last equation it is possible to deduce the allowed scattering events. We infer that no ordinary-to-ordinary transitions are possible since $N(O, O, \delta) = 0$ as \mathbf{e}_O is always perpendicular to \mathbf{n}_0 . Such a scattering may nevertheless be produced by fluctuations in the isotropic part of the dielectric tensor which, however, are much smaller than the director-induced scattering, and so we shall ignore it. Furthermore, Eq. (22) allows no forward scattering along the director. Notice also that—again adopting $K_\delta, \eta_\delta \propto S^2$ and $\varepsilon_a \propto S$ —the matrix element $B(\dots, t)$ depends weakly on the nematic order parameter S . Hence (quasi)elastic single light scattering is nearly independent of temperature T (the front factor $k_B T$ changes only slightly within the nematic phase). Such independence has indeed been observed (Chandrasekhar, 1977).

In the Born approximation under consideration, the structure factor is directly related to the differential scattering cross section giving the scattered energy per unit of time, unit solid angle element, and unit incident intensity in a medium of volume V (Langevin, 1974; Langevin and Bouchiat, 1975):

$$\begin{aligned} \frac{d\sigma}{d\Omega_k^\beta}(\alpha \hat{\mathbf{k}}_{\text{in}} \rightarrow \beta \hat{\mathbf{k}}_{\text{out}}) \\ = \frac{V}{(4\pi)^2} n_\alpha(\hat{\mathbf{k}}_{\text{in}}) \cos \delta_\alpha B(\alpha \hat{\mathbf{k}}_{\text{in}} \rightarrow \beta \hat{\mathbf{k}}_{\text{out}}) n_\beta^3(\hat{\mathbf{k}}_{\text{out}}). \end{aligned} \quad (23)$$

We have used here the solid-angle element $d\Omega_k^\beta$ associated with the outgoing wave vector. For extraordinary light, it differs from the solid-angle element $d\Omega_R^\beta$ associ-

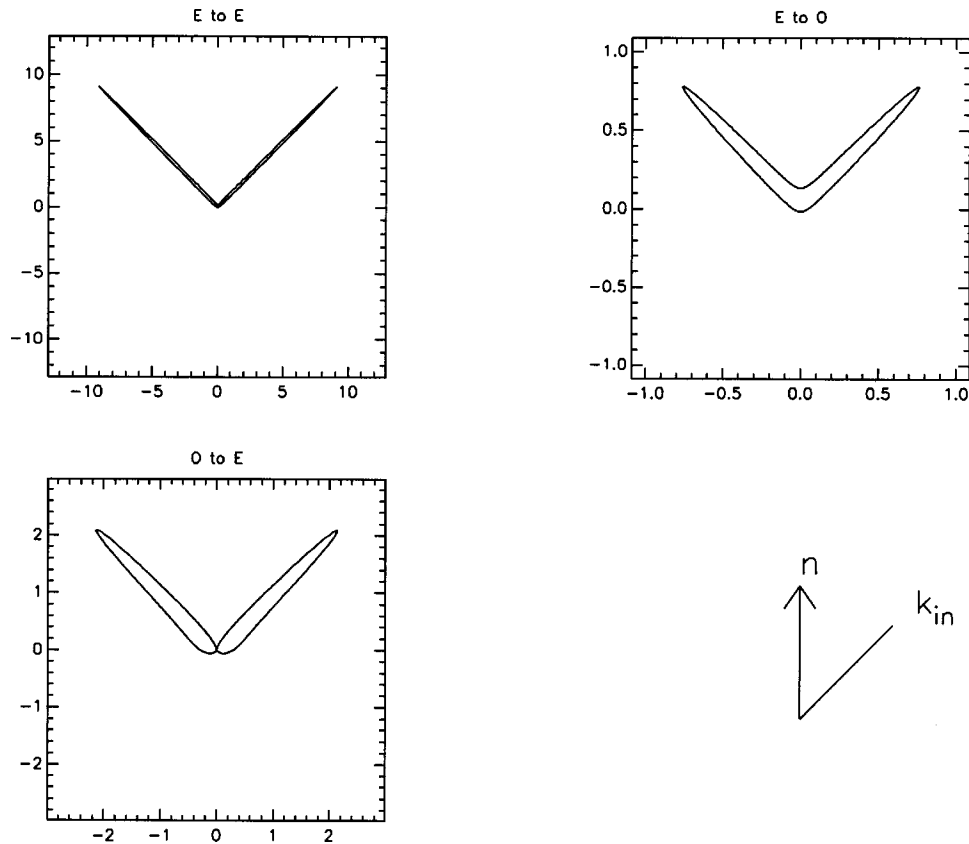


FIG. 3. Polar plots of the normalized phase functions (=differential cross section normalized to total cross section) for different polarization transitions as a function of the outgoing wave vector \mathbf{k}_{out} . The incident wave vector \mathbf{k}_{in} has been kept constant in the direction indicated together with the optical axis \mathbf{n} in the figure on the lower right. The phase function depends on the polar angles of \mathbf{k}_{in} and \mathbf{k}_{out} with the optical axis and on the azimuthal angle between the projections of the two wave vectors in the plane perpendicular to the optical axis. In the polar plot, the azimuthal angle has been integrated over, explaining the vertical mirror symmetry. The O - O phase function is identically equal to zero. The parameters correspond to the liquid crystal compound 5CB and a magnetic coherence length $\xi=5 \mu\text{m}$.

ated with the Poynting vector, being more relevant experimentally. The exact relation is discussed by Stark *et al.* (1997). In Fig. 3 we show polar plots of the phase function [defined as the differential cross section (23) normalized by the total cross section for a given incident direction, and thus a dimensionless number] for different polarization transitions. They will be important in the discussion of multiple scattering.

III. LIGHT DIFFUSION AND HIDDEN CONSEQUENCES OF ROTATIONAL SYMMETRY

In this section we want to look more closely at the link between single scattering and multiple scattering and to apply this knowledge to nematic liquid crystals. Radiative transfer is an old subject that goes back to the end of the last century, when astrophysicists (Schuster, 1905; see also Chandrasekhar, 1960) formulated the equation of radiative transfer. This equation describes in a phenomenological way how transport of particles takes place inside an inhomogeneous medium. In the equation of radiative transfer, light is thought of as made up of classical particles without phase. Despite its phenomenological nature, the algebraic structure is quite com-

plex, and its numerical solution is, even in a simple case, not straightforward (van de Hulst, 1980). The equation of radiative transfer models light transfer at length and time scales much larger than the wavelength and the period of light.

The equation can be derived microscopically (Sheng, 1995) by summing up the so-called ladder diagrams (see Fig. 6 below). It is an equation that can be solved for the so-called *specific intensity*, the intensity of light traveling in direction \mathbf{k} and being modulated in space and time. In Eq. (25) we shall define it rigorously as the Wigner distribution of the complex electric-field amplitude. We remark that the radiative transfer equation correctly describes single scattering when applied to thin samples. Its most severe restriction is the assumption of sufficiently weak scattering. The last criterion implies that the mean free path should be much longer than the wavelength.

The equation of radiative transfer has been used in nematic liquid crystals to study the first low orders of scattering (Romanov and Shalaginov, 1988). The analysis quickly becomes cumbersome and technical. Fortunately, the equation admits a dramatic simplification in the regime where multiple scattering dominates. It turns

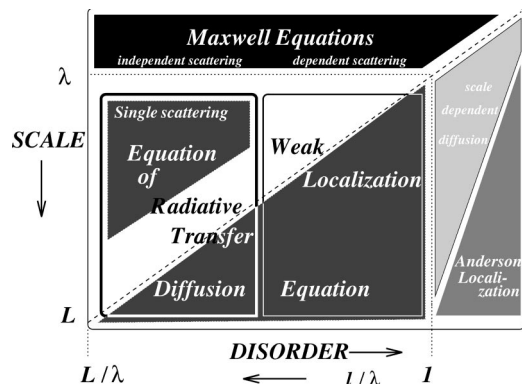


FIG. 4. Schematic diagram showing the different regimes in the transport theory of waves. On the horizontal axis is a typical parameter quantifying the amount of disorder in the system. The vertical axis represents the length scale of observation. It can be seen that the diffusion approximation covers a regime beyond the equation of radiative transfer. It breaks down at small length scales, roughly when the scale is comparable to the mean free path (the oblique dashed line), or at very large disorder where Anderson localization sets in. In the regime labeled “Weak Localization,” interference effects are important.

into a simple and familiar diffusion equation. The physical picture behind this simplification is a classical random walk of a “photon” from one scatterer to another.

There are three reasons why the diffusion approximation has become so popular. Experimentally, the diffusion approximation seems so far to be valid on scales all the way down to one mean free path (Li *et al.*, 1993). Theoretically, it gives ugly but closed-form formulas for transmission and reflection even for anisotropic scattering of vector waves in more sophisticated geometries (Li *et al.*, 1993). Finally, the diffusion approximation allows physicists to study multiple light scattering in a regime where the equation of radiative transfer does not apply. It is believed to be a genuine hydrodynamic limit of rigorous transport theory, including new aspects of interference, polarization, and scattering that are not contained in the equation of radiative transfer (see Fig. 4). The diffusion equation contains all information that has been left over after many scattering events in a very compact way.

In the diffusion approximation, the local energy current density $\mathbf{J}(\mathbf{r}, t)$ and the local energy density $\rho(\mathbf{r}, t)$ at time t are related by “Fick’s law,”

$$\mathbf{J}_i(\mathbf{r}, t) = -D_{ij} \partial_j \rho(\mathbf{r}, t). \quad (24)$$

The second-rank tensor D_{ij} is the diffusion tensor. It is instructive to discuss the restrictions imposed by all kinds of symmetry operations. Equation (24) can easily be checked on parity symmetry, where the current density and the gradient change sign. Time-reversal symmetry has been broken, but this symmetry is no longer a fundamental one once we deal with *ensemble-averaged* observables, as in Eq. (24). It is well known in transport theory that ensemble averaging destroys time-reversal symmetry (Grabert, 1982).

Rotational symmetry has been generally assumed in textbooks since it applies to typical media like milk, sugar, paint, and fog. In that case one necessarily arrives at an isotropic diffusion tensor: $D_{ij} = D \delta_{ij}$. Only one coefficient D remains, the diffusion constant. Up until about four years ago, no optical experiment ever needed to abandon this assertion of rotational symmetry. Today, anisotropic light diffusion is known not only in oriented nematic liquid crystals (Kao *et al.*, 1997) but also in light propagation in magnetic fields (Rikken and van Tiggelen, 1996; Sparenberg, Rikken, and van Tiggelen, 1997). Nematic liquid crystals are special because rotational symmetry is broken but translational symmetry is—statistically speaking—kept intact, allowing hopefully the definition (24) of a constant diffusion tensor once the liquid becomes larger than a mean free path.

In principle, the observable quantity in diffuse transport is the time-dependent specific intensity at some place \mathbf{r} inside or outside the medium, signifying the local current of energy per unit surface, per unit solid angle in the direction \mathbf{k} . It will of course also depend on the frequency ω of the light. Because we want to study polarization, we shall introduce a second-rank tensor $\Phi_{ij,\mathbf{k}}(\mathbf{r}, t)$ of the electric field components E_i .³ We define it as the \mathbf{q} -Fourier transform and Ω -Laplace transform of the field-field correlation function

$$\Phi_{ij,\mathbf{p},\omega}(\mathbf{q}, \Omega) \equiv \langle E_i(\mathbf{p} + \mathbf{q}/2, \omega + \Omega/2) E_j^* \times (\mathbf{p} - \mathbf{q}/2, \omega - \Omega/2) \rangle. \quad (25)$$

Mathematically this is recognized as a Wigner distribution. The microscopic variables ω and \mathbf{p} are associated with the fast oscillations of the wave packet in space and time. On the other hand, the macroscopic variables Ω and \mathbf{q} determine the propagation of the wave envelope, which is always orders of magnitude slower. This decoupling of frequencies is called the slowly varying wave approximation; a typical wave packet is shown in Fig. 5.

The equation of radiative transfer is a balance equation for $\Phi_{ij,\mathbf{k}}(\mathbf{r}, t)$, in the same way that the Boltzmann equation is a balance equation for the phase-space distribution $f(\mathbf{r}, \mathbf{v}, t)$ of classical particles. A difference between the two is that in normal Boltzmann theory the collisions take place among the particles, so that the collision term is bilinear in $f(\mathbf{v})$. In the radiative transfer equation, “photons” collide with fixed scattering centers and the collision term is linear in $\Phi_{ij,\mathbf{k}}$. The aim of diffusion theory is to express $\Phi_{ij,\mathbf{k}}(\mathbf{r}, t)$ in terms of *only* the energy density ρ and the total current density \mathbf{J} , related by Eq. (24). In terms of $\Phi_{ij,\mathbf{k}\omega}(\mathbf{r}, t)$, Maxwell’s equations imply that

$$\rho(\mathbf{r}, t) = \int \frac{d^3 p}{(2\pi)^3} \varepsilon_{ik} \Phi_{ki,\mathbf{p}\omega}(\mathbf{r}, t) \quad (26)$$

³The usual description in terms of four Stokes variables (van de Hulst, 1980) is inconvenient in the birefringent media that we envisage.

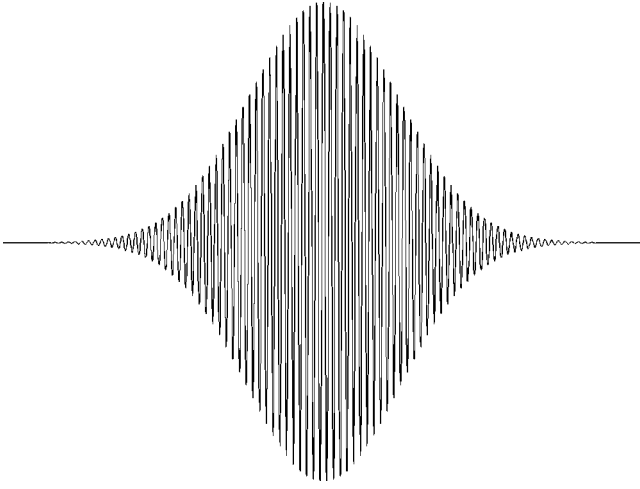


FIG. 5. Visualization of a typical wave packet obeying the slowly varying envelope approximation, either in time or in space. When this figure represents the pulse as a function of time, the rapid internal oscillations are denoted by the optical frequency ω , whereas the slowly varying envelope is characterized by a much smaller frequency Ω . Similarly, in real space, oscillations of the order of the optical wavelength are denoted by the wave number \mathbf{k} , and the smooth variation of the pulse itself by the much smaller wave number \mathbf{q} . The wave equation relates the rapid parameters ω and \mathbf{k} by means of a dispersion law, defining a wave velocity, whereas the diffusion equation relates the slow parameters Ω and \mathbf{q} by means of a diffusion constant.

$$J_n(\mathbf{r}, t) = \frac{c_0^2}{2\omega} \int \frac{d^3p}{(2\pi)^3} (2p_n \delta_{ik} - p_k \delta_{ni} - p_i \delta_{nk}) \times \Phi_{ki, \mathbf{p}\omega}(\mathbf{r}, t). \quad (27)$$

The expression for the current density J_n follows from the Poynting vector, $c_0(\mathbf{E} \times \mathbf{H})/4\pi$, together with one Maxwell equation to eliminate the magnetic field \mathbf{H} . Apart from polarization indices, both expressions look very much like the corresponding equations for number and current density in Boltzmann theory.⁴ It is anticipated that the momentum integrals pick up contributions only very near the constant-frequency shells $\omega_{e/o}(\mathbf{p}) = \omega$ in phase space where light propagation takes place.

In the case of rotational symmetry it is relatively easy to anticipate the relation between both macroscopic observables when light has reached the diffusion regime. The field-field correlation function depends on the energy density and current density as

$$\Phi_{ij, \mathbf{k}}(\mathbf{r}, t) \sim (\delta_{ij} - \hat{k}_i \hat{k}_j) \delta(\omega/v_p - k) \times [v_E \rho(\mathbf{r}, t) + 3\hat{k}_n J_n(\mathbf{r}, t) + \dots]. \quad (28)$$

⁴For a nonrelativistic particle with velocity \mathbf{v} , momentum divided by energy equals $m\mathbf{v}/mc_0^2$, whereas for a “photon” this amounts to $\hbar\mathbf{p}/\hbar\omega$. This suggests an analogy between the photon wave vector \mathbf{p} and the velocity \mathbf{v} . To make the analogy, replace \mathbf{p} by $(\omega/c_0^2)\mathbf{v}$. The expression for the current density J_n becomes similar to $\int d^3v f(\mathbf{v})\mathbf{v}$ in classical Boltzmann theory.

The Dirac delta distribution and the tensor in front make sure that only “on-shell” transverse photons propagate (i.e., frequency and wave number are related by the phase velocity v_p), as is physically required in isotropic media. The choice of current and energy density is such that Eq. (28) is consistent with definitions (26) and (27). The rest simply follows from rotational symmetry, leaving the tensor $D_{ij} = D\delta_{ij}$ in Eq. (24) and a scalar velocity v_E as arbitrary parameters to be obtained from a microscopic theory. The latter is only equal to the group velocity of the medium if the fluctuations in the dielectric tensor are small (van Tiggelen and Lagendijk, 1993). It is apparent from Eq. (28) that the radiation is unpolarized and a lot of information has been lost by multiple scattering. By inserting Eq. (24) into the angular expansion (28) we obtain

$$\Phi_{ij, \mathbf{k}}(\mathbf{r}, t) \sim v_E (\delta_{ij} - \hat{k}_i \hat{k}_j) \delta(\omega/v_p - k) \times [\rho(\mathbf{r}, t) - l^* \hat{k}_n \partial_n \rho(\mathbf{r}, t)]. \quad (29)$$

This relation defines a length scale l^* called the transport mean free path and relates it to the diffusion constant D according to the classical relation

$$D = \frac{1}{3} v_E l^*. \quad (30)$$

Equation (29) contains the start of a spatial Taylor expansion of $\rho(r - l^* \hat{h}, t)$. This implies $\Phi_{\mathbf{k}}(\mathbf{r}, t) \sim v_E \rho(\mathbf{r} - l^* \hat{\mathbf{k}}, t)$, i.e., the specific intensity is proportional to the energy density at a distance l^* along the line of sight (Browers and Deeming, 1984). This notion is very useful in interpreting the spectroscopy of the solar atmosphere, in particular because l^* depends on wavelength. Thus photons at different wavelengths originate from different depths and hence from regions with different temperatures.

The standard way to solve for the angular profile of the radiation emerging from a slab geometry is to add boundary conditions to the diffusion equation for the energy density ρ (Ishimaru, 1978). With respect to the direction θ of the net current \mathbf{J} , the angular profile is expected to be of the form $A + B \cos \theta$. For an arbitrarily polarized plane wave incident on a slab geometry with thickness L , one finds the *universal angular transmission* profile

$$T(\theta, L) = \frac{l^*}{L} \left(\frac{1}{2} + \frac{3}{4} \cos \theta \right), \quad (31)$$

independent of the precise phase function and polarization properties of the scatterers. Unfortunately, the diffuse angular profile does not contain any explicit information about the angular profile of one single scattering. All information is implicitly contained in the length l^* . The equation of radiative transfer relates it to the *extinction length* l according to

$$l^* = \frac{l}{1 - \langle \cos \theta_s \rangle} \equiv \gamma l. \quad (32)$$

Here $\langle \cos \theta_s \rangle$ is the average cosine of the scattering angle and clearly depends on the phase function. The dimensionless quantity γ has been introduced to make the connection later with the generalization of Eq. (32) to nematic liquid crystals. The transport velocity and the transport mean free path provide us with the only information left in the diffuse regime in rotationally isotropic media. For $\cos \theta > 0$, i.e., emergent radiation, Eq. (31) agrees to within a few percent with the exact solution of the equation of radiative transfer, for an arbitrary single-scattering function (see Fig. 11.2 of van de Hulst, 1980). The failure of the diffusion approximation is only apparent from the negative intensities it predicts when $\cos \theta < 0$, that is, for light sent back into the medium from transmission. But these directions are hardly ever measured, and this failure poses no interpretational problems.

IV. ANISOTROPIC LIGHT DIFFUSION IN NEMATICS

The spontaneously broken rotational symmetry in liquid crystals not only leads to birefringence in light propagation, but also implies the existence of hydrodynamic Goldstone modes (Forster, 1975), which we introduced earlier as director modes. Broken rotational symmetry will affect multiple scattering in several ways. Its most direct impact is upon the light propagation between two scattering events. Two modes of propagation with different group velocity and orthogonal polarization vectors determine the energy flow. In addition, broken rotational symmetry leads to three different elastic constants for the director fluctuations, which will—via the structure function in Eq. (20)—affect light scattering. Finally, director fluctuations are normal to the average director, leading to an anisotropy in the scattering function. The broken rotational symmetry is also responsible for the hydrodynamic nature of the director fluctuations (Chaikin and Lubensky, 1995), making their spatial correlations long range, as is apparent from Eq. (16). In general, multiple scattering of light close to phase transitions is an unexplored feature of radiative transfer.

It is our final aim to understand and to predict qualitatively and quantitatively all aspects of diffuse light in oriented nematics. In particular, we wish to relate these properties to the “amount of broken rotational symmetry,” quantified by the Maier-Saupe order parameter of the nematic phase. Because of the complexity of both the liquid crystal and the equation of radiative transfer, the much simpler diffusion approximation is a particularly attractive regime, although work has been done using the equation of radiative transfer in the small-angle approximation (Romanov and Shalaginov, 1988).

A. “Back-of-the-envelope” calculations

To obtain an order of magnitude for the diffusion constant of light in nematic liquid crystals, it is tempting to first ignore the orientational order of the liquid and to adopt a fully isotropic structure function, $B(\mathbf{q})$

$= (\omega/c_0)^4 \varepsilon_a^2 k T / K (q^2 + 1/\xi^2)$, which we refer to as the back-of-the-envelope model. The estimates obtained in this way will be given a subscript S to distinguish them from the rigorous calculation.

From Eq. (23), we recall that the single-scattering differential cross section for a small volume is basically proportional to $B(\mathbf{k}-\mathbf{k}')$ and the volume V itself (Berne and Pecora, 1976),

$$\frac{d\sigma}{d\Omega}(\mathbf{k} \rightarrow \mathbf{k}') = \frac{V}{(4\pi)^2} B(\mathbf{k}-\mathbf{k}'). \quad (33)$$

Given an incident flow I_{in} of photons per unit time and per unit surface, the total loss of energy per unit time is given by the angular integral of this expression, called the *total scattering cross section* σ . Hence the loss per unit surface is

$$\Delta I = -\frac{\sigma}{A} I_{\text{in}} = -\frac{\sigma}{V} \Delta z I_{\text{in}}, \quad (34)$$

where we have written $V = A \times \Delta z$. This formula suggests that the incident intensity decays as $\exp(-z/l_S)$, with the *scattering mean free path* or *extinction length* given by

$$\frac{1}{l_S} = \int \frac{d\Omega'_k}{(4\pi)^2} B(\mathbf{k}-\mathbf{k}'). \quad (35)$$

Upon doing the integral, we find for our simplified structure function

$$l_S = \frac{4\pi K c_0^2 \varepsilon}{\varepsilon_a^2 \omega^2 k T \ln(1 + 4\omega^2 \xi^2 \varepsilon / c_0^2)}. \quad (36)$$

For typical values (ξ is several μm in a magnetic field of 1 T) this gives the value $l_S \approx 0.1$ mm. This value is much larger than the correlation length ξ so that the conventional and popular picture of a sequence of single-scattering events seems to apply. As a matter of fact, the inequality $l_S \gg \xi$ can be verified even close to the (discontinuous) nematic-isotropic phase transition. The reason is that l_S depends weakly on the order parameter, whereas $\xi \sim \sqrt{S}$. Only in a magnetic field as small as 10^{-2} T (100 G) would the magnetic correlation length be of the order of 0.1 mm and become comparable to the extinction length. In the hypothetical case of vanishing magnetic field, the extinction length l_S goes to zero logarithmically in H . In this regime, the weak-scattering approximation apparently breaks down due to the long-range nature of the director fluctuations.

One can explicitly show that the amount of energy scattered by one director fluctuation of volume ξ^3 relative to the incoming light energy equals $\xi^3/4l_S$. This means that the weak-scattering approximation breaks down for $\xi \approx l_S$. Equivalently, to assure the weak-scattering approximation one must have $\xi \ll l_S$, which then suggests the picture of subsequent scattering from different director modes. To understand light scattering in a nematic with $\xi \approx l_S$, one has to go beyond the weak-scattering approximation. At the same time, one loses the familiar picture that light is scattered from different director modes at different places.

Due to long-range correlations, most of the scattering contained in l_S^* is in the forward direction. According to radiative transport theory, the length relevant in diffusion is the transport mean free path (32), which gives more weight to forward scattering than to backscattering. One finds

$$l_S^* = \frac{8\pi c_0^2 K \varepsilon}{\varepsilon_a^2 \omega^2 k T}, \quad (37)$$

weakly dependent on H as long as $\xi \geq 1 \mu\text{m}$. We obtain the much larger value of 1–5 mm, a length that corresponds to the transport mean free path of very dilute colloidal suspensions. A very convenient property of the length l_S^* is that it is not expected to be very sensitive to changes in the nematic order parameter, since as a rule of thumb $K \sim S^2$ and $\varepsilon_a \sim S$ (Chandrasekhar, 1977).

1. Equipartition of polarization in the diffuse regime

The model discussed above suffers badly from the neglect of broken rotational symmetry and its impact on polarization. Nevertheless, the following “educated guess” can be made to estimate one aspect of broken rotational symmetry. For a given frequency ω , the diffusion process tends to *equipartition* the electromagnetic energy among all microstates in the phase space of wave vectors allowed by the dispersion law $\omega(\mathbf{k})$. The spectral function counts the electromagnetic energy density in a phase-space cell (\mathbf{r}, \mathbf{p}) . In an infinite medium this density is on average independent of the space variable \mathbf{r} . For weak disorder it reads

$$\rho_{ij}^n(\omega, \mathbf{p}) = \hat{e}_i^n(\mathbf{p}) \hat{e}_j^n(\mathbf{p}) \delta[\omega - \omega_n(\mathbf{p})]. \quad (38)$$

Here \hat{e}^n denotes the normalized polarization vector of polarization mode n . If the disorder increases, the dispersion law $\omega_n(\mathbf{k})$ will achieve an uncertainty inversely proportional to the mean free time $\tau^n \approx l^n/v^n$ between two scattering events. By an exact sum rule (Mahan, 1981), the sum over all polarizations together with the integral over all frequencies of $\rho_{ij}^n(\omega, \mathbf{p})$ must be a constant independent of \mathbf{p} and independent of statistical parameters like temperature or density of scatterers. Equation (38) obeys this sum rule, and since the polarization has unit norm, this constant equals unity.

The total number of microstates (per unit volume) for polarization mode $n = e/o$ becomes

$$\rho_{e,o}(\omega) = \int \frac{d^3p}{(2\pi)^3} \text{Tr} \boldsymbol{\rho}^{e/o}(\omega, \mathbf{p}) = \frac{1}{8\pi^3} \int \frac{d^2S_{e,o}}{|\mathbf{v}_{ge,o}|}. \quad (39)$$

Here $d^2S_{e,o}$ is the surface element in \mathbf{k} space for both constant-frequency surfaces (Ashcroft and Mermin, 1976). The integration can be performed, and the result is simply

$$\frac{\rho_e}{\rho_o} = \frac{\varepsilon_{\parallel}}{\varepsilon_{\perp}}. \quad (40)$$

Despite the heuristic argument, this result is an *exact* outcome of transport theory (Stark and Lubensky, 1996; van Tiggelen, Maynard, and Heiderich, 1996). It gener-

ally holds when modes with different velocities are combined in a diffusion process. For that reason it applies for elastic waves in solid media (Weaver, 1982) and was recently observed in earthquake seismograms (Campillo, Margerin, and Shapiro, 1999). It can be seen that for negative anisotropies ($\varepsilon_a < 0$) ordinary waves dominate, whereas for $\varepsilon_a > 0$ extraordinary waves are in the majority. These results hold *regardless* of the exact selection rules for polarization transitions during the scattering process. This conclusion will be important in understanding the outcome of detailed calculations qualitatively.

2. Dynamic correlations

In Sec. II.C we reviewed the dynamics of director fluctuations in nematic liquid crystals. In the past this was studied extensively using the quasielastic light-scattering technique (Orsay Liquid Crystal Group, 1969; Chandrasekhar, 1977), which consists of measuring the small frequency shift of the (singly) scattered light due to the dynamics of the director modes. Measurements in the time domain have also been employed (see, for example, Mertelj and Copic, 1997). The dynamic time correlation function has been described in Eq. (15) and shows the competition of elastic and viscous forces. The typical time scale is given by γ/Kq^2 , with K a typical value for the elastic constants, $\mathbf{q} = \mathbf{k}_{\text{out}} - \mathbf{k}_{\text{in}}$ the scattering vector, and γ the Leslie rotational viscosity coefficient. In near forward scattering $q \ll \omega/c$, and the relaxation time is much larger than $10 \mu\text{m}$, even of the order of milliseconds.

During the last 10 years, quasielastic light-scattering experiments have been generalized to multiple scattering in colloidal suspensions. Multiple scattering from n scatterers makes a measurement typically \sqrt{n} times more sensitive for phase shifts that occur due to the motion of the scatterers. As a result, one can study very small time scales, much smaller than the one in single scattering. Work by Maret and Wolf (1987) demonstrated the utility of this so-called *diffusing wave spectroscopy* to monitor all sorts of hydrodynamic processes with many potential applications (Weitz and Pine, 1992; Boas, Campell, and Yodh, 1995).

Diffusing wave spectroscopy has recently been applied to aligned nematic liquid crystals (Kao *et al.*, 1997; Stark *et al.*, 1997) in both reflection and transmission. Detailed theoretical analyses have been made, incorporating polarization, different elastic modes, and all Leslie viscosities (Stark and Lubensky, 1996; Kao *et al.*, 1997; Stark and Lubensky, 1997; van Tiggelen, Heiderich, and Maynard, 1997). To simplify the analyses, we neglect all these complications and adopt the following time correlation function:

$$B(\mathbf{q}, t) = \frac{\omega^4 \varepsilon_a^2 k_B T}{c_0^4 K q^2} \exp\left(-\frac{K q^2 t}{\gamma}\right), \quad (41)$$

which replaces Eq. (21). It ignores polarization, anisotropic elasticity, anisotropic viscous effects, and finite

spatial correlations due to a magnetic field. What will change in multiple scattering when this explicit time dependence is considered?

Nothing, of course. Light moves much faster than the motion of the fluctuation and every photon sees a frozen director configuration while traveling through the medium. The time dependence of the medium generates a complete ensemble average every few microseconds. To resolve dynamics, one should look not at the average intensity but rather at the time-dependent correlation function $\langle I(0)I(t) \rangle$ either in reflection or in transmission. Assuming Gaussian statistics, this correlation directly relates to the electric-field autocorrelation function, according to

$$\langle I(0)I(t) \rangle = \langle I \rangle^2 + |\langle E(0)E^*(t) \rangle|^2. \quad (42)$$

This equation calls for a theory for $\langle E(0)E^*(t) \rangle$, which differs only slightly from the basic observable Φ in Eq. (25), since it involves fields measured at different times. In fact, in a rare case one has direct access to the field correlation function (Kao, Yodh, and Pine, 1993).

As soon as one considers the correlator $\langle E(t)E^*(t') \rangle$, the scattering cross section to be used should be $B(\mathbf{q}, t-t')$. The fields $E(t)$ and $E(t')$ both travel through a frozen medium, but this medium has changed in between the measurements. The time difference $t-t'$ is imposed by the measurement and can be chosen much smaller than the typical hydrodynamic relaxation time of the director correlations. For single scattering, there would be no substantial decay in the temporal electric-field correlations. However, because of the cumulative effect of all the scattering events along one light path, there is a relevant dephasing of the fields, which leads to a decay of the temporal electric-field correlations with which a dephasing length can be associated. Using Eq. (35), this dephasing length l_ϕ can be calculated as

$$\frac{1}{l_\phi(t)} = \int \frac{d\Omega'_k}{(4\pi)^2} [B(\mathbf{k}-\mathbf{k}', 0) - B(\mathbf{k}-\mathbf{k}', t)]. \quad (43)$$

The integration can be done for our simple model (41). For times $t < \tau_c \equiv c_0^2 \gamma / 4K\omega^2 \varepsilon$ (where τ_c is the relaxation time of a director mode with wave number $q = 2\omega/c$), i.e., less than a few microseconds, the exponential can be expanded and the result is

$$\frac{1}{l_\phi(t)} = \frac{\varepsilon_a^2 \omega^4 k_B T}{4\pi \gamma c_0^4} \times t. \quad (44)$$

This is the standard result also obtained from more sophisticated calculations (Stark and Lubensky, 1997; van Tiggelen, Heiderich, and Maynard, 1997). Note that the dephasing is independent of the elastic constant K . For times beyond τ_c , it can be seen that $B(t) \rightarrow 0$ so that, using Eq. (43) we find that $l_\phi(t)$ converges to the extinction length l_S , which equals a fraction of a millimeter. Before the time τ_c , the dephasing time is much larger.

As long as the dephasing length is large compared to the transport mean free path ($t \ll \tau_c$), it can be built into standard diffusion theory as a small perturbation (Ishi-

maru, 1978). The diffusion equation for $\Phi(\mathbf{r}, t) \equiv \langle E(\mathbf{r}, 0)E^*(\mathbf{r}, t) \rangle$ can be written as

$$\left[-\frac{1}{3} v_E l_S^*(t) \nabla^2 + \frac{v_E}{l_\phi(t)} \right] \Phi(\mathbf{r}, t) = \text{source}, \quad (45)$$

i.e., a conventional diffusion equation with time-dependent diffusion constant $v_E l_S^*(t)/3$ and time-dependent absorption rate $v_E/l_\phi(t)$ for the field correlations. The time-dependent transport mean free path is usually not considered but should, strictly speaking, be obtained from $B(\mathbf{q}, t)$ and not $B(\mathbf{q}, 0)$. Using Eq. (32),

$$\begin{aligned} \frac{1}{l_S^*(t)} &= \int \frac{d\Omega'_k}{(4\pi)^2} (1 - \cos \theta) B(\mathbf{k}-\mathbf{k}', t) \\ &= l_S^*(0) \frac{1 - \exp(-t/\tau_c)}{t/\tau_c}, \end{aligned} \quad (46)$$

with $l_S^*(0)$ given by Eq. (37). This implies that at times beyond τ_c the transport mean free path relevant for time correlation is enlarged by a factor t/τ_c . The consideration of a time-dependent mean free path starts to be relevant at times comparable to τ_c .

The solution of the diffusion equation in transmission through a slab with thickness L is well known to be

$$\Phi(\text{Trans}, t) = \langle T(0) \rangle \frac{L/L_\phi}{\sinh(L/L_\phi)}, \quad (47)$$

where a new dephasing length L_ϕ is introduced by $L_\phi = \sqrt{l^*} l_\phi / 3$. It can be interpreted as an absorption length for the time correlations of diffusing light. We emphasize that L_ϕ is not an absorption length. It just shows up as if it were an absorption length in the diffusion. Our simple model gives $L_\phi^{-1} \sim \sqrt{t}$ at times short compared to τ_c . Equation (47) holds when $l_a \gg l_s$, which is equivalent to $t \ll \tau_c$. As long as $L < L_\phi$, this means that $\ln \Phi(\text{Trans}, t) \sim -t/t_T$, going over into $\ln \Phi \sim \ln(t/t_T) - \sqrt{t/t_T}$ as $L > L_\phi$ at longer times, both of course subject to the constraint $t < \tau_c$. This is plainly true, since the typical diffusing wave spectroscopy time in transmission is $t_T \approx (l^*/L)^2 \tau_c \ll \tau_c$. In reflection from a semi-infinite medium, one finds $\Phi(\text{Ref}, t) \sim \exp(-\sqrt{t/t_R})$ (Pine *et al.*, 1990). Note that the typical time t_R in reflection is much greater than t_T . It is actually comparable to τ_c . This means that the concept of a “time-dependent transport mean free path,” as discussed above, might not be totally irrelevant in reflection. Diffusing wave spectroscopy has been successfully applied to the study of dynamic director fluctuations in the compound 5CB (Kao *et al.*, 1997; Stark *et al.*, 1997).

B. Rigorous transport theory

The final aim of transport theory is to calculate the relation between the incident intensity and the thermodynamically ensemble-averaged outgoing intensity, starting from the wave equation underlying the scattering processes in a random medium. In the present case of light propagation in liquid crystals, we deal with the Maxwell equations, and we have already analyzed single

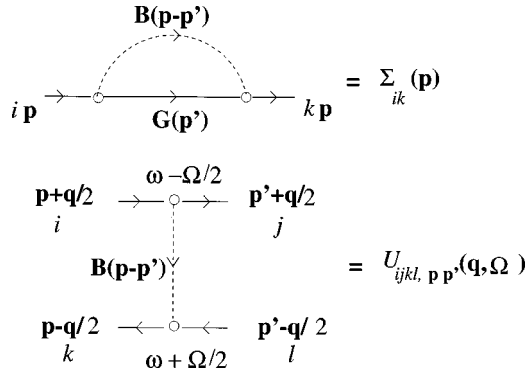


FIG. 6. Diagrammatic Feynman representation of the operator L , defined in Eq. (50), relating incoming and outgoing intensity and polarization. The bottom line denotes the propagation of the complex conjugated electric field, and therefore it is directed in the opposite direction. Open circles denote a thermal fluctuation $\delta\varepsilon$. The bold horizontal lines represent the Dyson Green's function, which gives the scattered field from one thermal fluctuation to the other. Dashed vertical lines connect correlated fluctuations.

scattering, which is supposed to be an essential building block in multiple scattering.

The observable quantity $\Phi_{ik,\mathbf{p}}^{\text{out}}(\mathbf{r}, t)$ was defined earlier in Eq. (25). It is most convenient first to assume full translational symmetry and then to add boundaries later. Since we neglect any nonlinear response, the relation between incident and outgoing light must be linear. Upon Fourier transforming space variables and Laplace transforming time variables, this relation can be written as

$$\Phi_{ik,\mathbf{p}}^{\text{out}}(\mathbf{q}, \Omega) = \int \frac{d^3 p'}{(2\pi)^3} L_{ijkl,\mathbf{p}\mathbf{p}'}(\mathbf{q}, \Omega) \Phi_{jl,\mathbf{p}'}^{\text{in}}(\mathbf{q}, \Omega). \quad (48)$$

In real space this would take the form of a space/time convolution. In Fig. 6 we explain the conventions in the diagrammatic presentation of the tensor $L_{ijkl,\mathbf{p}\mathbf{p}'}$.

1. Reciprocity and flux conservation

Before getting into more precise calculations, it is instructive to discuss the basic properties of the tensor \mathbf{L} . We have stated already that time-reversal symmetry is destroyed by ensemble averaging. However, reciprocity should still be intact. The reciprocity principle guarantees the existence of an equivalence principle between detector and source (Born and Wolf, 1975; van de Hulst, 1980). Expressed algebraically, this reads

$$L_{ijkl,\mathbf{p}\mathbf{p}'}(\mathbf{q}, \Omega) = L_{jilk,-\mathbf{p}'-\mathbf{p}(-\mathbf{q}, \Omega). \quad (49)$$

A second important property of the tensor \mathbf{L} is a general result of transport theory. In the presence of energy or particle conservation, a transport quantity like L_{ijkl} is expected to exhibit *hydrodynamic* behavior (Forster, 1975). The hydrodynamic regime is characterized by the so-called Kubo limit $\Omega \rightarrow 0$ and $\mathbf{q} \rightarrow 0$, i.e., long time and length scales. In particular, one has

$$L_{ijkl,\mathbf{p}\mathbf{p}'}(\mathbf{q}, \Omega) \rightarrow \frac{w_{ki}(\mathbf{p}, \mathbf{q}) w_{jl}(\mathbf{p}', \mathbf{q})}{-i\Omega + \mathbf{q} \cdot \mathbf{D} \cdot \mathbf{q} + \mathcal{O}(\Omega^2, q^3)}. \quad (50)$$

It is not difficult to see that in real space this equation implies a diffusion equation for the photon density $\rho(\mathbf{r}, t)$, obtained from the second-rank tensor $\Phi_{ij}^{\text{out}}(\mathbf{r}, t)$ by means of Eq. (26). The symmetric numerator of Eq. (50) is imposed by the reciprocity principle (49). More formally, it is possible to consider the second-rank tensor $w_{jl}(\mathbf{p}, \mathbf{q})$ as the eigenfunction of the fourth-rank tensor $L_{ijkl,\mathbf{p}\mathbf{p}'}(\mathbf{q}, \Omega)$, corresponding to the hydrodynamic eigenvalue $1/(-i\Omega + \mathbf{q} \cdot \mathbf{D} \cdot \mathbf{q})$ (Barabanenkov and Ozrin, 1995; Barabanenkov, Zurk, and Barabanenkov, 1995). Eigenfunctions are usually needed in one order lower than the order of perturbation considered for the eigenvalue. For that reason $w_{jl}(\mathbf{p}, \mathbf{q})$ is independent of Ω and contains at most a bilinear form (\mathbf{p}, \mathbf{q}) . A linear factor \mathbf{q} corresponds in real space to a space gradient, and this brings us to a rigorous foundation for Eq. (29), but now generalized to arbitrary complex systems. The replacement of L by its hydrodynamic limit at all length and time scales is the diffusion approximation. In isotropic systems, the second-rank tensor $w_{ki}(\mathbf{p}, \mathbf{q})$ must be proportional to $\delta_{ik}[A + B(\mathbf{p} \cdot \mathbf{q})]$, which brings us back to Eq. (28). In the presence of a homogeneous magnetic field \mathbf{B} , a magneto-optical contribution of the form $\det(\mathbf{B}, \mathbf{p}, \mathbf{q}) \delta_{ik}$ is allowed by symmetry and induces a photon Hall effect (Lacoste and van Tiggelen, 1999). In nematic liquid crystals the three independent vectors \mathbf{n}_0 , $\mathbf{e}_o(\mathbf{p})$, and $\mathbf{e}_e(\mathbf{p})$ are available to construct the tensor $w_{ki}(\mathbf{p}, \mathbf{q})$.

2. Dyson's equation in nematics

To describe light propagation in random media, the first quantity to consider is the Green's function for the electric field. It is a second-rank tensor describing the propagation of the field from one place to another,

$$\mathbf{G}(\omega, \mathbf{r}, \mathbf{r}') = \left\langle \mathbf{r} \left| \frac{1}{\omega^2 \boldsymbol{\varepsilon}(\mathbf{x}) / c_0^2 - \mathbf{p}^2 + \mathbf{p} \otimes \mathbf{p} + i0} \right| \mathbf{r}' \right\rangle. \quad (51)$$

The dielectric tensor $\boldsymbol{\varepsilon}$ has a random component, over which we shall perform an ensemble average, and an anisotropic deterministic component, both according to Eqs. (1) and (3). In the nematic phase, ensemble averaging over thermal fluctuations of the director restores translational symmetry. It is thus convenient to consider the Fourier transform of the ensemble average $\langle \mathbf{G}(\omega, \mathbf{r}, \mathbf{r}') \rangle$,

$$\mathbf{G}(\omega, \mathbf{p}) = \frac{1}{\omega^2 \boldsymbol{\varepsilon}_0 / c_0^2 - \mathbf{p}^2 + \mathbf{p} \otimes \mathbf{p} + \boldsymbol{\Sigma}(\omega, \mathbf{p})}, \quad (52)$$

in which the average thermal fluctuations are contained in the Dyson self-energy $\boldsymbol{\Sigma}$; due to broken rotational symmetry $\boldsymbol{\Sigma}$ explicitly depends on the direction of the wave vector \mathbf{p} with respect to the optical axis. The weakness of thermal fluctuations guarantees the validity of the Born approximation for this object, as known from conventional perturbation theory (Frisch, 1968),

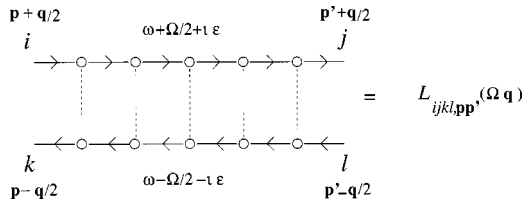


FIG. 7. Diagrammatic Feynman representation of the self-energy Σ and the irreducible vertex \mathbf{U} , defined in Eqs. (55) and (59). Feynman diagrams are usually depicted in momentum representation. The “dangling” lines denote incoming or outgoing plane waves whose momentum labels and polarization indices have been added. The open circles indicate two scattering events from a director fluctuation mode with wave vector $\mathbf{p}-\mathbf{p}'$, correlated by the structure function \mathbf{B} . The symbol \mathbf{G} is the Green’s tensor representing the propagation of light in between two director fluctuations. Note the transfer of momentum from light to matter, with momentum conservation at each point. Iteration of the Bethe-Salpeter equation (58) using the vertex \mathbf{U} shown here generates the ladder diagrams shown in Fig. 7.

$$\Sigma_{ik}(\omega, \mathbf{p}) = \int \frac{d^3 p'}{(2\pi)^3} B_{ijkl}(\mathbf{p}-\mathbf{p}') G_{jl}(\omega, \mathbf{p}'). \quad (53)$$

A diagrammatic representation of this dominant term to the self-energy is shown in Fig. 7. The structure function $B_{ijkl}(\mathbf{q})$ associated with the thermal fluctuations was introduced earlier in Eq. (20), and in the previous section we argued that only the static version is needed here. Since the fluctuations are weak, the three eigenvectors that diagonalize \mathbf{G} will still be to a good approximation the electric polarization vectors $\mathbf{e}_{e,o,l}$ of the host medium, introduced in Sec. II.A. However, the three corresponding indices of refraction n_α will have changed, achieving both a real and an imaginary part. The longitudinal mode is not relevant to our discussion. For the two propagating modes, the extinction length can be defined as

$$l_{elo}(\hat{\mathbf{p}}) = \frac{k_{elo}}{-\text{Im} \Sigma_{elo}(\hat{\mathbf{p}})}, \quad (54)$$

in terms of the matrix element $\Sigma_{elo}(\hat{\mathbf{p}}) \equiv \hat{\mathbf{e}}_{elo}(\hat{\mathbf{p}}) \cdot \Sigma(\omega, \mathbf{k}_{elo}) \cdot \hat{\mathbf{e}}_{elo}(\hat{\mathbf{p}})$. This matrix element can easily be evaluated numerically (Val’kov and Romanov, 1986; Heiderich, Maynard, and van Tiggelen, 1997). The above definition of extinction length is the microscopic foundation of the heuristic reasoning that led us earlier to Eq. (35). The Dyson Green’s function is the mathematical object that corresponds to the remnant of the incident field, sometimes called the “coherent beam.”

The Green’s function now takes the form of a dyadic,

$$\mathbf{G}(\omega, \mathbf{p}) = \frac{\hat{\mathbf{e}}_o(\hat{\mathbf{p}}) \otimes \hat{\mathbf{e}}_o(\hat{\mathbf{p}})}{k_o^2 - p^2 + ik_o/l_o(\hat{\mathbf{p}})} + \frac{\hat{\mathbf{e}}_e(\hat{\mathbf{p}}) \otimes \hat{\mathbf{e}}_e(\hat{\mathbf{p}})}{\cos^2 \delta_e [k_e^2(\hat{\mathbf{p}}) - p^2] + ik_e(\hat{\mathbf{p}})/l_e(\hat{\mathbf{p}})} + \text{longitudinal}, \quad (55)$$

where $\hat{\mathbf{e}}_{o,e}$ denotes unit polarization vectors. In Fig. 8 we

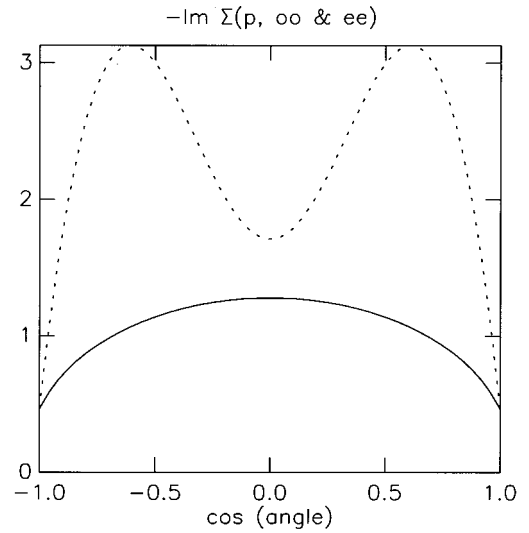


FIG. 8. Imaginary part of the self-energy (in units of $\varepsilon_a^2 \omega^3 k_B T / 8\pi K_3 c_0^3 \varepsilon_\perp$, per unit area) for extraordinary waves (ee , dashed) and ordinary waves (oo , solid) as a function of the angle between the wave vector and the optical axis. This quantity is inversely proportional to the extinction length. The parameters chosen are consistent with the nematic liquid crystal 5CB, shown in Table I, and a magnetic coherence length $\xi = 5 \mu\text{m}$. Along the optical axis ($\cos = \pm 1$) both polarizations degenerate and the self-energies coincide. The graph is symmetric about $\cos = 0$ because of the mirror symmetry with respect to planes perpendicular to the optical axis.

show the imaginary part of the self-energy for both polarizations. We took the optical and hydrodynamical values known for the nematic 5CB (see Table I). It can be seen that both depend on the angle of propagation. For the ordinary waves this perhaps surprising result (recall that these modes have an isotropic dispersion law) is due to the inhibition of direct ordinary-ordinary $O-O$ scattering, which requires an intermediate and anisotropic extraordinary wave excitation. In Fig. 9 we show the imaginary part of the self-energies for the *hypothetical* case in which $\varepsilon_a \rightarrow 0$ and $K_1 = K_2 = K_3$, i.e., no kinematical or elastic anisotropy at all. This figure demonstrates the sole impact of the intrinsic anisotropy of the director fluctuations on the extinction length. It is a hypothetical case since $\varepsilon_a = 0$ also implies that $l_e = l_o = \infty$. It can be deduced that the extinction length for ordinary waves is smallest in all directions. This is a result of the absence of $O-O$ scattering. Furthermore, for both polarizations, the mean free path is largest along the optical axis. First, this is due to the fact that no forward scattering is allowed along the optical axis, as stated earlier. Second, light modes traveling along the director are always ordinary and can therefore only be scattered into extraordinary (E) waves.

3. Bethe-Salpeter equation in nematics

The Dyson Green’s function describes the propagation of the ensemble-averaged field in the presence of scattering. To understand the impact of scattering on the

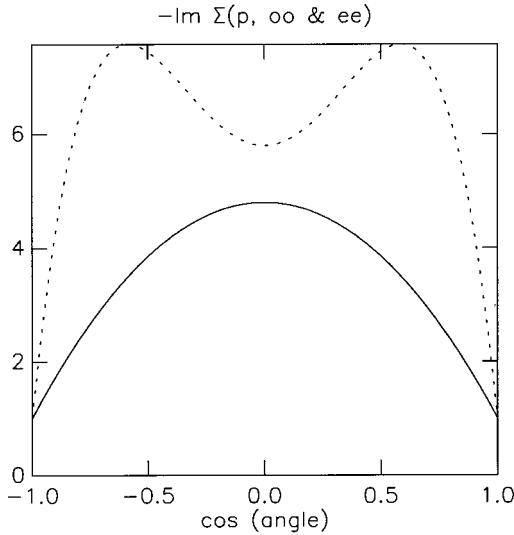


FIG. 9. As in Fig. 8 (with the same units for the self-energy), but now for the hypothetical case in which $\varepsilon_a = 0$ and all elastic constants are the same. The anisotropy is now due only to the thermal fluctuations perpendicular to the optical axis, and not to birefringence or elasticity. This case is purely academic in the sense that the unit for the self-energies defined in the previous figure vanishes, but it shows the impact of the anisotropic director fluctuations on the angular dependence of the extinction mean free path, without being modified by anisotropic elasticity and uniaxial birefringence.

ensemble-averaged intensity, one needs to consider the product of two Green's functions. Similar to the Dyson equation (52) defining the self-energy, one can write an equation for the two-photon Green's function, thereby introducing a new object. This equation is called the Bethe-Salpeter equation. Formally it reads (Barabanenkov and Ozrin, 1995; Barabanenkov, Zurk, and Barabanenkov, 1995; Sheng, 1995; van Rossum and Nieuwenhuizen, 1999)

$$\langle \mathbf{G}_1 \otimes \mathbf{G}_2^* \rangle = \langle \mathbf{G}_1 \rangle \otimes \langle \mathbf{G}_2^* \rangle + \langle \mathbf{G}_1 \rangle \otimes \langle \mathbf{G}_2^* \rangle \cdot \mathbf{U}_{12} \cdot \langle \mathbf{G}_1 \otimes \mathbf{G}_2^* \rangle. \quad (56)$$

The labels 1 and 2 usually correspond to different nearby frequencies and wave vectors, similar to the basic observable Φ_{ijkl} introduced in Eq. (48). They can also correspond to two different times of measurement, as is customary in diffusing wave spectroscopy techniques for probing time correlations in wave diffusion (Maret, 1997). The new object \mathbf{U} that has been introduced—called the *irreducible vertex*—is a fourth-rank tensor. Its advantage is that it has much in common with what one would call a “differential cross section” in the equation of radiative transfer. The ensemble-averaged two-photon Green's function $\langle G_{ij} G_{lk}^* \rangle$ is basically equal to the tensor L_{ijkl} defined in Eq. (48). It enables us to calculate specific intensities anywhere at any time, given a source.

It is not our purpose to give the detailed theory here, and we should like to refer the interested reader to published material (Frisch, 1968; Sheng, 1995; Lagendijk and van Tiggelen, 1996; POAN Research Group, 1998).

An old and difficult problem—even for simple systems—is how and under what conditions one can transform the Bethe-Salpeter equation into the familiar equation of radiative transfer (Papanicolaou and Burridge, 1975). If we forget about technical details, the radiative transfer equation follows from Bethe-Salpeter in the weak-scattering approximation. A more specific problem for complex media like those with broken rotational symmetry is the calculation of the diffusion asymptotics, as was made explicit in Eq. (50). For isotropic systems this last problem has basically been solved.

In nematic liquid crystals the easy part is the choice of the vertex tensor \mathbf{U} . Since scattering is very weak, the Born approximation for scattering from “one thermal fluctuation” is going to be the building block for multiple scattering. Translating to momentum space (Fig. 6), we have

$$U_{ijkl}(\mathbf{k}_1, \mathbf{k}_2, \mathbf{k}_3, \mathbf{k}_4) \rightarrow \delta(\mathbf{k}_1 - \mathbf{k}_2 - \mathbf{k}_3 + \mathbf{k}_4) \times \frac{\omega^4}{c_0^4} \langle \delta\varepsilon_{ik}(\mathbf{k}_1 - \mathbf{k}_2) \delta\varepsilon_{jl}(\mathbf{k}_3 - \mathbf{k}_4) \rangle. \quad (57)$$

The Dirac delta function ensures that momentum is conserved. It is a natural consequence of translational symmetry of the ensemble-averaged random medium.

The basic technique in diffusion theory is to find the eigenvalue closest to zero of the Bethe-Salpeter equation (Barabanenkov and Ozrin, 1991; Barabanenkov and Ozrin, 1995; Stark and Lubensky, 1997; van Tiggelen, Heiderich, and Maynard, 1997). The actual calculation for a nematic has been carried out using numerical iteration (van Tiggelen, Maynard, and Heiderich, 1996) and using spherical harmonic expansion (Stark and Lubensky, 1996), with numerically identical results. At infinite length scales—that is, $\mathbf{q} = \mathbf{0}$ in Eq. (48)—this hydrodynamic eigenvalue must be exactly zero because of energy conservation laws (Mahan, 1981).

An exact result of transport theory is that the eigenfunction associated with this eigenvalue is the so-called spectral function $\rho_{ij}^n(\omega, \mathbf{p})$ of the system,

$$\Phi_{ij, \mathbf{p}}(\mathbf{q} = 0) \propto \sum_{n=e,o} \rho_{ij}^n(\omega, \mathbf{p}). \quad (58)$$

This function was been introduced earlier in Eq. (38) for a nematic liquid crystal. Now being a second-rank tensor, it must be the generalization of the term ρ in Eq. (29). Equation (58) expresses the effect of diffusion to drive the system toward equipartition of energy over phase space. As was put forth heuristically in Eq. (40), this process is subject to a constant-frequency constraint.

Second-order Rayleigh-Schrödinger perturbation theory in \mathbf{q} transforms the eigenvalue zero into the bilinear form $D_{ij} q_i q_j$, where D_{ij} can be identified with the diffusion tensor. The latter turns out to be given by a vector generalization of the Kubo-Greenwood formula (Barabanenkov and Ozrin, 1991), known for electrons in disordered semiconductors (Mahan, 1981) and in that

case often obtained by linear response theory. At the same time, the eigenfunction associated with the diffuse mode achieves a perturbational bilinear form $\Gamma_{nm}k_nq_m$, which provides the generalization of the term $k_n\partial_n$ in Eq. (29). The actual calculation of the tensors D_{ij} and Γ_{ij} is facilitated by the following *controlled* approximations:

- (1) Interference between E and O waves can be neglected. In multiple scattering this holds true when the dephasing of O and E modes between two successive collisions is large, i.e., $|k_E - k_O|l \gg 1$, with k the wave number. This criterion easily follows since the distance of the two excitations in Eq. (58) in phase space is $|k_E - k_O|$, whereas their typical size is of the order of $1/l$. The present criterion guarantees that the two excitations do not overlap in phase space. Because the extinction length l is so much larger than the wavelength (roughly $100 \mu\text{m}$), this inequality is obeyed even near the nematic-isotropic phase transition. This transition is weakly first order so that a finite-order parameter (and thus a finite value for $k_E - k_O$) remains near T_c . Note that around the optical axis the two excitations always overlap. The volume of overlap in phase space is small compared to the total hemisphere and is therefore negligible for multiple scattering.
- (2) The correlation length ξ of the director fluctuations is less than the mean free path. Most nematic liquid crystals are placed in a magnetic field (typically 1 T) to get them aligned, and this inequality ($\xi \approx 5 \mu\text{m}$, $l \approx 0.1 \text{ mm}$) is well satisfied.

The first approximation in particular makes nematic liquid crystals very attractive as a multiple-scattering medium. It implies that the two polarization modes are unaware of each other during propagation and only couple during the scattering from a thermal fluctuation. Moreover, since such scatterings prohibit OO transitions, any O wave must change abruptly into an E wave after each scattering event. In isotropic media, on the other hand, two opposite polarizations are degenerate and any intermediate (elliptical) polarization can be formed. The second approximation implies that multiple light scattering in a nematic liquid crystal can actually be envisaged as a sequence of single-scattering events, as is true in milk and fog. When $\xi > l$ this familiar picture will be lost, and the theory becomes more involved (van Tiggelen, Heiderich, and Maynard, 1997). We stress that the second criterion emphasizes weak scattering, which simplifies the numerical evaluation of the diffusion constants, and that it is *not* a criterion for the existence of diffusion.

The two approximations simplify the the Kubo formula for the diffusion tensor enormously. What remains is a relatively simple expression for the diffusion tensor involving a wave-number integral over the E and O constant-frequency surfaces, familiar from the theory of electron-impurity scattering in the solid state. One final subtlety remains. In conventional isotropic media the

transport mean free path l^* (appearing in the diffusion constant) and the extinction length l (determining the exponential decay of the coherent signal) are related by Eq. (32). They differ in the weight of their forward scattering ($\cos \theta = 1$). For a nematic liquid crystal this factor is definitely going to be important since the scattering function is proportional to $1/(\mathbf{k}_{\text{in}} - \mathbf{k}_{\text{out}})^2$. Moreover, it is not necessarily a number, but depends on polarization. The final Kubo formula for the diffusion tensor reads (van Tiggelen, Heiderich, and Maynard, 1997)

$$\mathbf{q} \cdot \mathbf{D} \cdot \mathbf{q} = \frac{1}{(2\pi)^3 \rho(\omega)} \sum_{n=e,o} \int \frac{d^2 S_n}{|\mathbf{v}_{gn}|} l^n(\mathbf{k}_n) \times (\mathbf{v}_{gn} \cdot \mathbf{q}) \gamma^n(\hat{\mathbf{k}}_n, \mathbf{q}), \quad (59a)$$

with the associated eigenfunction [see Eq. (50)]

$$w_{ij}^n(\mathbf{k}, \mathbf{q}) = \rho_{ij}^n(\omega, \mathbf{k}_n) [1 + i l^n(\mathbf{k}_n) \gamma^n(\hat{\mathbf{k}}_n, \mathbf{q})]. \quad (59b)$$

In this equation, $d^2 S_n$ denotes the surface element on the frequency surface n and \mathbf{v}_{gn} the group velocity of mode n , being the normal vector of the constant-frequency surface S_n ; $l^n(\mathbf{k}_n)$ is the extinction length for the polarization n in the direction \mathbf{k}_n (Val'kov and Romanov, 1986; Kuz'min, Romanov, and Zubkov, 1994; Heiderich, Maynard, and van Tiggelen, 1997), given explicitly by Eq. (54). The factor $\rho(\omega)$ stands for the number of microstates per unit volume defined in Eq. (39).

The bilinear form $\gamma^n(\mathbf{k}_n, \mathbf{q})$ is the generalization of the scalar number γ in Eq. (32). It can be calculated from the phase functions and the polarization selection rules (van Tiggelen, Heiderich, and Maynard, 1997). In Fig. 3 we showed the phase functions associated with the three allowed polarization transitions. The large forward scattering gives γ^n an often large positive value, as was already obvious from the scalar relation (32). The uniaxiality and the special selection rules for OO scattering in a nematic liquid crystal lead to

$$\gamma^n(\mathbf{k}, \mathbf{q}) = A_n(\vartheta)(\mathbf{k} \cdot \mathbf{q}) + \frac{1}{2} B_n(\vartheta)(\mathbf{n}_0 \cdot \mathbf{k})(\mathbf{n}_0 \cdot \mathbf{q}) - (\mathbf{k} \cdot \mathbf{e}_n)(\mathbf{q} \cdot \mathbf{e}_n). \quad (60)$$

This involves four even functions of the angle ϑ between wave vector and optical axis, rather than one simple scalar number γ . Broken rotational symmetry leaves a considerable fingerprint in the multiple-scattering process.

In an alternative method for the calculation of the diffusion constants one expands the eigenfunction w_{ij}^n , discussed earlier, in modified spherical harmonics Y_m^l . The great advantage of this method is that it provides simple perturbational expressions that have been checked to apply with satisfying accuracy. In this method, the hydrodynamic eigenvalue $-i\Omega + \mathbf{q} \cdot \mathbf{D} \cdot \mathbf{q}$ with the two diffusion constants D_{\parallel} and D_{\perp} is determined perturbatively. This can be done within the Green's-function formalism (Stark and Lubensky, 1996, 1997) by using the equation of radiative transfer (Stark, 1998) or by directly summing up the different light paths (Stark *et al.*, 1997). Due to the uniaxial symmetry of the nematic phase, D_{\parallel} and D_{\perp} are related to the azimuthal

quantum numbers $m=0$ and $m=\pm 1$, respectively. The special choice of the modified spherical harmonics establishes a sequence of approximations labeled by odd-angular-momentum quantum numbers l . Stark and Lubensky (1997) showed that $l=1$ spherical harmonics already give a very good approximation for D_{\parallel} and D_{\perp} . Addition of the $l=3$ basis functions generally results in changes of less than 1%. For $l=1$, we give the explicit formulas for D_{\parallel} and D_{\perp} (Stark *et al.*, 1997; Stark, 1998), which can easily be programmed on a personal computer,

$$D_{\parallel} = \frac{8\pi}{9} \frac{c_0}{n_o^2 n^3} \times \frac{\mathcal{B}_{ee}^{\parallel} + \mathcal{B}_{oo}^{\parallel} - 2\mathcal{B}_{eo}^{\parallel}}{\mathcal{B}_{ee}^{\parallel} \mathcal{B}_{oo}^{\parallel} - (\mathcal{B}_{eo}^{\parallel})^2}, \quad (61)$$

$$D_{\perp} = \frac{8\pi}{9} \frac{c_0}{n_o^2 n^3} \times \frac{\mathcal{B}_{ee}^{\perp} + \mathcal{B}_{oo}^{\perp} \varepsilon_{\perp}/\varepsilon_{\parallel} - 2\mathcal{B}_{eo}^{\perp} \sqrt{\varepsilon_{\perp}/\varepsilon_{\parallel}}}{\mathcal{B}_{ee}^{\perp} \mathcal{B}_{oo}^{\perp} - (\mathcal{B}_{eo}^{\perp})^2}, \quad (62)$$

where we have introduced the ‘‘parallel’’ matrix elements [with unit one over length, and by Eq. (35) typically equal to the inverse mean free path $1/l_S$],

$$\begin{aligned} \mathcal{B}_{ee}^{\parallel} &= \int_{-1}^1 dC_{ek} \int_{-1}^1 dC_{eq} \int_0^{2\pi} \frac{d\varphi_{\mathbf{kq}}}{2\pi} \\ &\quad \times (C_{ek}^2 - C_{ek} C_{eq}) B(e\hat{\mathbf{k}} \rightarrow e\hat{\mathbf{q}}) \\ &\quad + \frac{\varepsilon_{\perp}}{\varepsilon_{\parallel}} \int_{-1}^1 dC_{ek} \int_{-1}^1 dC_{oq} \int_0^{2\pi} \frac{d\varphi_{\mathbf{kq}}}{2\pi} \\ &\quad \times C_{ek}^2 B(e\hat{\mathbf{k}} \rightarrow o\hat{\mathbf{q}}), \\ \mathcal{B}_{oo}^{\parallel} &= \frac{\varepsilon_{\perp}}{\varepsilon_{\parallel}} \int_{-1}^1 dC_{ok} \int_{-1}^1 dC_{eq} \int_0^{2\pi} \frac{d\varphi_{\mathbf{kq}}}{2\pi} \\ &\quad \times C_{ok}^2 B(o\hat{\mathbf{k}} \rightarrow e\hat{\mathbf{q}}), \\ \mathcal{B}_{eo}^{\parallel} &= - \int_{-1}^1 dC_{ek} \int_{-1}^1 dC_{oq} \int_0^{2\pi} \frac{d\varphi_{\mathbf{kq}}}{2\pi} \\ &\quad \times C_{ek} C_{oq} B(e\hat{\mathbf{k}} \rightarrow o\hat{\mathbf{q}}). \end{aligned} \quad (63)$$

The unit vector $\hat{\mathbf{k}}$ is determined by its polar angle $\vartheta_{\mathbf{k}}$ and its azimuthal angle $\varphi_{\mathbf{k}}$ in the frame with the director as the z axis. We abbreviated $C_{ok} \equiv \cos \vartheta_{\mathbf{k}}$ for the ordinary waves, and $C_{ek} = n_e(\hat{\mathbf{k}}) \cos \vartheta_{\mathbf{k}} / n_o$ for the extraordinary waves. In both cases the modified spherical harmonics $C_{n\mathbf{k}}$ ranges between -1 and 1 . To carry out the integration above, the structure function $B(\alpha\hat{\mathbf{k}} \rightarrow \beta\hat{\mathbf{q}})$ must be expressed in terms of $C_{\alpha\mathbf{k}}$ (see Appendix C of Stark and Lubensky, 1997). Due to the uniaxial symmetry of the nematic phase, one azimuthal integration can be trivially extracted, leaving a second one over $\varphi_{\mathbf{qk}} \equiv \varphi_{\mathbf{q}} - \varphi_{\mathbf{k}}$ that can actually be handled analytically (Stark and Lubensky, 1997). We recall that the azimuthal average of the structure function B was displayed earlier in Fig. 3.

The ‘‘perpendicular’’ matrix elements \mathcal{B}^{\perp} can be calculated similarly, by making replacements in the

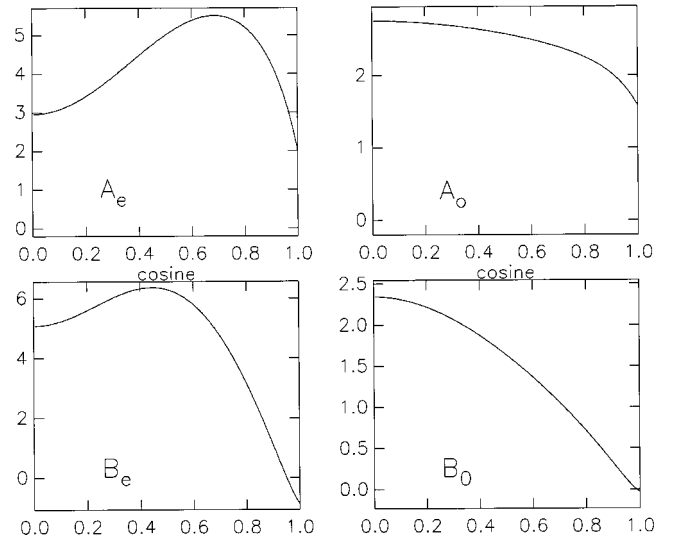


FIG. 10. Numerical solution for the four functions in Eq. (60) as a function of (the cosine of) the angle with respect to the optical axis. These four functions generalize the factor $1 - (\cos \theta)^{-1}$, which distinguishes extinction and transport mean free path in an isotropic medium. We choose $\varepsilon_a/\varepsilon_{\perp} = 0.228$, equal elastic constants for splay and twist distortions, but a larger bend elastic constant $K_3/K_2 = 2.3$. The correlation length amounts $\xi = 1.8 \mu\text{m}$. These values correspond roughly to the liquid crystal compound 5CB. The diffusion anisotropy is calculated to be $D_{\parallel}/D_{\perp} = 1.51$.

integrands $\frac{C_{e/o\mathbf{k}}^2(1 - C_{e/o\mathbf{k}}^2)/2}{\sqrt{1 - C_{e/o\mathbf{k}}^2} \sqrt{1 - C_{e/o\mathbf{q}}^2} \cos \varphi_{\mathbf{kq}}/2}$ and $C_{e/o\mathbf{k}} C_{e/o\mathbf{q}} \rightarrow \sqrt{1 - C_{e/o\mathbf{k}}^2} \sqrt{1 - C_{e/o\mathbf{q}}^2} \cos \varphi_{\mathbf{kq}}/2$. Again, one azimuthal integration has been carried out (Stark and Lubensky, 1997). The cube of the refractive indices $\bar{n}^3 = \frac{1}{2} \varepsilon_{\perp}^{1/2} (\varepsilon_{\parallel} + \varepsilon_{\perp})$ has been averaged over both constant frequency surfaces.

4. Qualitative discussions

Figure 10 shows the four functions A_E , A_O , B_E , and B_O defined in Eq. (60), calculated for the liquid crystal 5CB. This calculation relies on a ‘‘two-constant approximation’’ that adopts equal Frank elastic constants for splay (K_1) and twist (K_2) distortion. For $K_3/K_{1,2} = 2.3$ the theoretical prediction is $D_{\parallel}/D_{\perp} = 1.51$. For the actual values $K_3/K_2 = 2.3$ and $K_3/K_1 = 1.27$ of 5CB one finds the value $D_{\parallel}/D_{\perp} = 1.45$ (Stark and Lubensky, 1996, 1997). These values are consistent with the experimental result 1.60 ± 0.25 (Kao *et al.*, 1997). The enhanced diffusion along the optical axis is caused by both the positive dielectric anisotropy (see below) and the relatively large bend elastic constant. The absolute value of the diffusion constant is expressed as $D_{\parallel,\perp} = d_{\parallel,\perp} \times 8\pi c_0^3 K_1 \sqrt{\varepsilon_{\perp}} / 3kT \varepsilon_a^2 \omega^2$ where the unit comes from the ‘‘back-of-the-envelope’’ result in Eq. (32).⁵ For 5CB the

⁵The mean free path units l_B^* used by van Tiggelen, Heiderich, and Maynard (1997) and l_0^* used by Stark and Lubensky (1997) differ by the factor $9K_3/8K_1$. This unit depends weakly on order parameter.

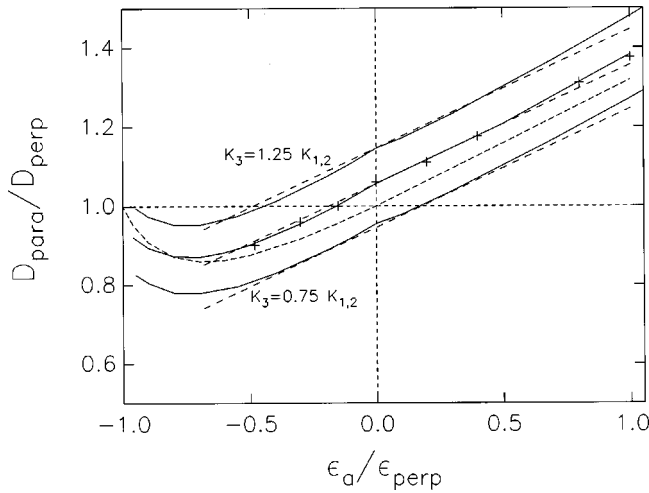


FIG. 11. Diffusion anisotropy as a function of the uniaxial dielectric anisotropy. The middle solid line corresponds to the calculation of van Tiggelen, Maynard, and Heiderich (1996) for an isotropic free energy; the other two assume equal strength of splay and twist distortion, but a different bend strength. The fine dashed line through the center represents the kinematic anisotropy predicted by Eq. (64). The + symbols denote calculations by Stark and Lubensky (1997) based on a more accurate formula than Eq. (63) since $l \leq 3$ spherical harmonics were included. The three parallel dashed lines denote the Taylor expansion given in Eq. (123) of Stark and Lubensky (1997). It was derived from the approximate formula (63). The correlation length is fixed at $5 \mu\text{m}$ but a change would hardly affect the figure.

value $d_{\parallel} = 1.7$ is obtained, leading to $D_{\parallel} = 1.5 \times 10^9 \text{ cm}^2/\text{sec}$. The reported experimental value is $0.7 \times 10^9 \text{ cm}^2/\text{sec}$ (Kao *et al.*, 1997; Stark *et al.*, 1997). It was determined by matching the average transmission of a liquid-crystal cell to the transmission of a colloidal suspension with known l^* .

In Fig. 11 we show the anisotropy D_{\parallel}/D_{\perp} of the diffusion constants parallel and perpendicular to the optical axis as a function of the dielectric anisotropy ϵ_a of the host medium. A convenient property of this ratio is that $\epsilon_a = \epsilon_{\parallel} - \epsilon_{\perp}$ is the only parameter really sensitive to the order parameter of the nematic phase (the dependency of the elastic constants $K_i \sim S^2$ cancels). As a result this graph gives a good impression of what is predicted for the anisotropy in diffusion as the Maier-Saupe order parameter changes.

Since most people know that the diffusion constant is a product of velocity and mean free path, an often posed question is which one is more important for the diffuse anisotropy. As we mentioned earlier, *three* sources exist for anisotropy in diffusion: the birefringence of the host medium, the director fluctuations that only occur perpendicular to the optical axis, and the anisotropic free energy of the nematic liquid crystal. Only the first one addresses the velocity, whereas all three affect the mean free path.

The influence of elasticity has been discussed in great detail by Stark and Lubensky (1997). One finds that both D_{\parallel} and D_{\perp} increase with increasing Frank elastic

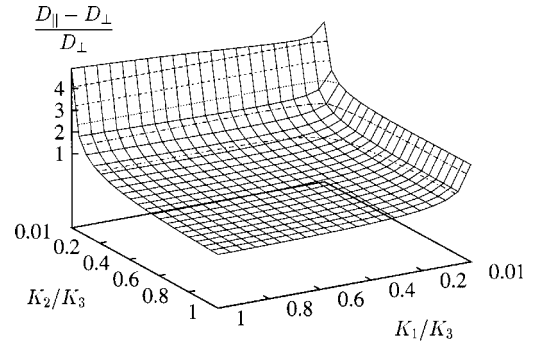


FIG. 12. Relative anisotropy $(D_{\parallel} - D_{\perp})/D_{\perp}$ as a function of K_1/K_3 and K_2/K_3 for $\epsilon_a = 0$.

constants since the light scattering from the director fluctuations decreases. There is an asymmetry between splay and twist distortions. Both diffusion constants decrease more strongly with increasing K_2/K_3 . Figure 12 shows the anisotropy $(D_{\parallel} - D_{\perp})/D_{\perp}$ as a function of K_1/K_3 and K_2/K_3 . It grows when the elastic constants are reduced, showing that D_{\perp} is more affected by splay and twist distortions than is D_{\parallel} . The asymmetry between splay and twist is clearly visible. The figure covers the range of thermotropic calamitic nematics where $K_1/K_3 < 1$ and $K_2/K_3 < 1$.

The sole impact of birefringence can be revealed by ignoring both the angular dependence of the self-energy in Eq. (54) and the scattering phase functions. This implies that $A_n = 1$ and $B_n = 0$ so that $\gamma^n(\mathbf{k}_n, \mathbf{q}) \rightarrow (\omega/c_0)(\mathbf{v}_{gn} \cdot \mathbf{q})/|\mathbf{v}_{gn}|^2$, with \mathbf{v}_{gn} the group velocity of polarization mode n . This approximation transforms the Kubo formula for the diffusion tensor into a “cheap but popular” formula often encountered in solid-state books, where it is used to estimate the influence of band structure on electron conductivity without bothering about the phase function of the impurities [see, for example, Eq. (13.25) of Ashcroft and Mermin, 1976]. The simplification makes the anisotropy in diffusion equal to the *kinematic anisotropy* associated with the birefringence,

$$D_{ij} \propto \sum_{n=e,o} \int \frac{d^2 S_n}{|\mathbf{v}_{gn}|} (\hat{\mathbf{v}}_{gn})_i (\hat{\mathbf{v}}_{gn})_j \left(\sum_{n=e,o} \int \frac{d^2 S_n}{|\mathbf{v}_{gn}|} \right)^{-1} \\ \equiv \frac{1}{3} p \delta_{ij} + (1-p) n_{0i} n_{0j}. \quad (64)$$

The surface element $dS_n/|\mathbf{v}_{gn}|$ counts the local number density of modes in phase space, as specified earlier in Eq. (39). The second equality defines the variable $0 < p < 1$ quantifying the effective dimensionality: $p = 1$ indicates an isotropic 3D system, whereas $p = 0$ would imply a 1D system along the optical axis \mathbf{n}_0 . Equation (64) would give $D_{\parallel}/D_{\perp} = -2 + 3/p$. The fine dashed line in Fig. 11 shows that this approximation captures the trend of the exact calculation quite well. The other two mechanisms for the anisotropy—selection rules and elasticity—cause this curve to shift along the vertical axis. Pure kinematic anisotropy is likely to persist if the scattering is caused by isotropic point scatterers, and not

by thermal director fluctuations. For this reason this approximation may apply to so-called filled monodomain nematics, i.e., oriented nematic liquid crystals containing dispersed colloidal particles (Kreuzer, Tschudi, and Eidschink, 1992; Bellini *et al.*, 1998). However, a clear experiment would require the director field around the particles to be only weakly perturbed, to reduce light scattering from the nonuniform director field. This can be achieved by weak anchoring of the director at the surface of the particle and by applying a magnetic field.

The kinematic approximation of Eq. (64) obviously fails to capture the strong dependence of the anisotropy in diffusion on the elastic constants, which come in only via the phase function. This limitation is evident for the compound 5CB where Eq. (64) would give $D_{\parallel}/D_{\perp} = 1.07$ (experiment: 1.6 ± 0.2), clearly underestimating the impact of anisotropic elastic constants. Even for elastic isotropy $K_1 = K_2 = K_3$, the approximation fails to provide the nontrivial value $D_{\parallel}/D_{\perp} = 1.056$ as $\varepsilon_a \approx 0$ (Stark and Lubensky, 1996; van Tiggelen, Maynard, and Heiderich, 1996). The somewhat larger diffusion along the optical axis is explained by the fact that the extinction length is largest along the optical axis, as is evident from Fig. 9. This anisotropy in the scattering would be compensated for by a negative birefringence $\varepsilon_a/\varepsilon_{\perp} = -0.15$, for which the diffusion would be isotropic. It would be interesting to observe this effect in discotic nematics, which possess a negative ε_a . The three parallel dashed lines in Fig. 11 confirm the good quantitative agreement between the different approaches followed by van Tiggelen, Maynard, and Heiderich (1996) and Stark and Lubensky (1996).

The overall tendency in Fig. 11 can be understood in the following way. In Eqs. (39) and (40) we calculated the total number of photons E or O . For positive dielectric anisotropies ($\varepsilon_{\parallel} > \varepsilon_{\perp}$), the extraordinary waves E dominate the energy. Their constant-frequency surface is flattened along the optical axis, and as a result most of them propagate with the larger component of the group velocity along the optical axis \mathbf{n}_0 , suggesting that $D_{\parallel} > D_{\perp}$. For very negative dielectric anisotropy, ordinary waves O dominate, and the diffusion anisotropy is suppressed since the group velocity of O waves is isotropic. This simplified argument does not acknowledge the inhibition of direct O - O scattering, which requires an intermediate—and hence anisotropic— E wave, but it explains why, for large negative anisotropies, the diffusion tensor becomes nearly isotropic.

The anisotropy in diffusion, as well as the absolute values of the diffusion constants, are influenced very little by the correlation length ξ (Stark and Lubensky, 1997). This can be verified easily in the back-of-the-envelope model, where ξ comes in only logarithmically. Only when $\xi \gg l$ (corresponding to a magnetic field of less than 100 gauss) would significant modifications start to appear, since our second approximation would be violated. This value is so small that we can safely extrapolate the theory towards zero magnetic field. Figure 13 shows the dependence of the diffusion tensor on the magnetic field.

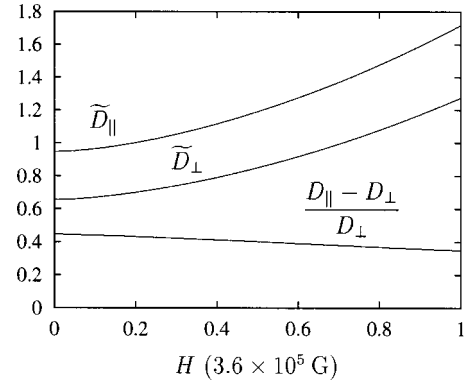


FIG. 13. Reduced diffusion constants \tilde{D}_{\parallel} , \tilde{D}_{\perp} (i.e., normalized to the numerical value $3\pi c_0^3 K_3 \sqrt{\varepsilon_{\perp}} / (k_B T \varepsilon_a^2 \omega^2)$), and relative anisotropy $(D_{\parallel} - D_{\perp})/D_{\perp}$ as a function of magnetic field. The material parameters correspond to the liquid crystal compound 5CB. The diffusion constants increase with the magnetic field since the light scattering from director fluctuations decreases with H . The relative anisotropy is hardly affected by the field.

C. Diffuse transmission from a nematic cell

The eigenfunction corresponding to the eigenvalue with long-range diffusion provides all information at long length scales. The diffusion approximation consists of using this eigenfunction at *all* length scales. Obviously this is an approximation for length scales comparable to, say, the transport mean free path. Yet because of its simplicity this approximation is widely used and gives surprisingly accurate fits to experiments (Li *et al.*, 1993).

In real space, the macroscopic wave vector \mathbf{q} becomes a space gradient. After Fourier transformation of the hydrodynamic eigenfunction $w_{ij}(\mathbf{p}, \mathbf{q})$ in Eq. (59b), the specific intensity tensor becomes

$$\Phi_{ij,\mathbf{p}}(\mathbf{r}) \propto \sum_{n=e,o} \rho_{ij}^n(\omega, \mathbf{p}) \times \{ \rho(\mathbf{r}) - l^n(\mathbf{p}) \gamma^n(\hat{\mathbf{p}}, \nabla) \rho(\mathbf{r}) \}. \quad (65)$$

The spectral function $\rho_{ij}^n(\omega, \mathbf{p})$ was defined in Eq. (38). This is the desired generalization of Eq. (29) to a nematic liquid crystal. Upon solving the diffusion equation for a slab of thickness L , one can find the polarization and current at any point in the medium. For a continuous-wave point source and a slab, which is infinitely extended perpendicular to the slab normal, the equal-intensity lines in transmission are ellipses with aspect ratio $x/y = \sqrt{D_{xx}/D_{yy}}$.

In Fig. 14 we show a calculation for the angular transmission coefficient of a nematic cell, given plane-wave illumination, and adopting the parameters known for 5CB. It is confirmed that the emergent radiation deviates from the universal law (31) in isotropic media and is polarized since, at any angle, more E than O photons emerge. So far, no experiments have been performed to verify these statements and, in particular, to verify the validity of the diffusion approximation as it comes to its nontrivial predictions for polarization and angular transmission profiles in anisotropic media.

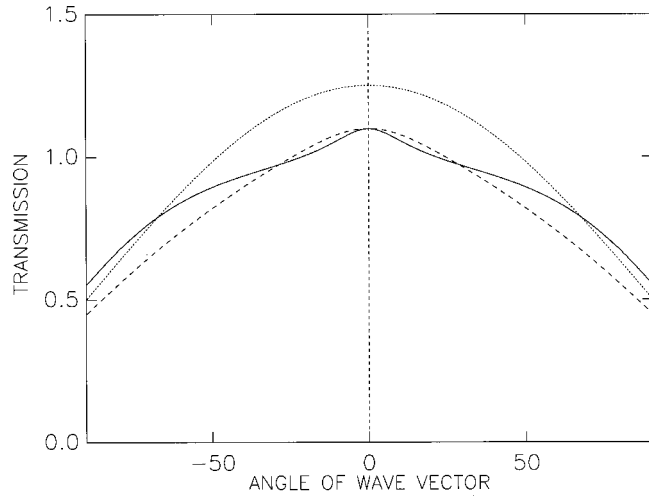


FIG. 14. Theoretical prediction for the angular transmission profiles $T(\theta)$ of diffuse extraordinary (solid) and ordinary (dashed) light from a slab filled with the liquid crystal compound 5CB, according to the diffusion approximation. The angle θ corresponds to the angle of the wave vector with respect to the slab normal (and not that of the group velocity, which would be different for different polarizations). The nematic director is chosen normal to the slab, i.e., at $\theta=0$. The dotted line shows the universal law $0.5+0.75 \cos \theta$ for isotropic media. No birefringent refraction has been treated at the interface.

The total transmission coefficient, summed over polarization and angle, can easily be obtained from Eq. (65) and the Kubo formula (59a). If the z axis is chosen to be the normal of the slab, the result is

$$T(L) = \frac{4D_{zz}/v_E}{L + 4D_{zz}/v_E}, \quad (66)$$

where we have introduced the diffusion constant $D_{zz} = \hat{\mathbf{z}} \cdot \mathbf{D} \cdot \hat{\mathbf{z}}$ for diffusion along the slab normal. It is physically plausible that the transmission T is proportional to D_{zz} . It is also plausible that T is inversely proportional to the length L of the slab: this is just the familiar Ohm's law, saying that the resistance is proportional to the length L . However, T being a number between 0 and 1, D_{zz} must for dimensional reasons be divided by some "transport" velocity v_E , similar to Eq. (28), but which is here *a priori* not evident due to birefringence. The diffusion approximation (65) gives

$$v_E(\mathbf{n}_0 \cdot \hat{\mathbf{z}}) = 2 \sum_{n=e,o} \int \frac{d^2 S_n^+}{|\mathbf{v}_{gn}|} (\mathbf{v}_n \cdot \hat{\mathbf{z}}) \left(\sum_{n=e,o} \int \frac{d^2 S_n^+}{|\mathbf{v}_{gn}|} \right)^{-1} \\ = \begin{cases} c_0 / \sqrt{\varepsilon_{\perp}} & \mathbf{z} \parallel \mathbf{n}_0 : \text{homeotropic cell} \\ c_0 [\sqrt{\varepsilon_{\parallel}} + \sqrt{\varepsilon_{\perp}}] / [\varepsilon_{\parallel} + \varepsilon_{\perp}] & \mathbf{z} \perp \mathbf{n}_0 : \text{planar cell.} \end{cases} \quad (67)$$

The first equality involves a weighted average of the normal component of the group velocity over both frequency surfaces $d^2 S_n^+$. The + indicates that the integration takes place over the part where this normal component points towards transmission. This result is a consequence of the two-stream model on which the dif-

fusion approximation relies, making a difference only between photons propagating to the left or to the right. In the second equality the integration is carried out for two specific geometries. The fact that the transport velocity depends on the orientation of the optical axis can be seen as the manifestation of birefringence in light diffusion. This leads to the interesting and perhaps unexpected prediction that

$$\frac{T_{\perp}}{T_{\parallel}} \neq \frac{D_{\perp}}{D_{\parallel}}. \quad (68)$$

There is an ambiguity in the definition of the transport mean free path in a nematic liquid crystal. It is plausible to define two transport mean free paths according to $D_{\perp} = \frac{1}{3} v_E(\perp) l_{\perp}^*$ and $D_{\parallel} = \frac{1}{3} v_E(\parallel) l_{\parallel}^*$. Equation (66) then would take the form of Ohm's classical law $T(\parallel, \perp) = 4 l_{\parallel, \perp}^* / 3L$, which makes the transport mean free paths directly accessible by experiment. This has so far not been done.

V. CONCLUSIONS AND FUTURE PROSPECTS

This review has aimed to sum up the theoretical state of the art in describing diffuse light in nematics. These systems constitute a concrete example in which radiative transfer can be studied under complex conditions. In isotropic systems radiative transfer is very well studied, both theoretically and experimentally. Diffusion approximations, numerical methods like adding-doubling methods (de Haan, Bosma, and Hovenier, 1987), and Monte-Carlo simulations (van Albada and Lagendijk, 1987; Martinez and Maynard, 1994; Heiderich, Maynard, and van Tiggelen, 1997; Kao *et al.*, 1997; Stark *et al.*, 1997; Margerin *et al.*, 1998) have covered the whole regime from single scattering to infinite scattering and have studied most novel aspects, such as polarization, coherent backscattering, and correlation functions. Recent studies have concentrated on very dense systems that can no longer be described by ordinary radiative transfer theory.

More and more attention has been focused on complex aspects of wave diffusion. Among other complex systems, aligned nematic liquid crystals constitute a new challenge for radiative transfer. The interest of these systems lies in their orientational anisotropy, which can be controlled externally and which is quantified by the Maier-Saupe order parameter S . The disadvantage is the weakness of their thermal fluctuations, whose orientational anisotropy has several nontrivial consequences for multiple light scattering, such as the anisotropy of the diffusion tensor of the light, the angular distribution of the transmitted light, and the equipartition of different polarizations in the diffuse regime. Recent experiments—either stationary or time resolved—have confirmed the existence of anisotropic diffusion (Kao *et al.*, 1997; Wiersma *et al.*, 1999).

Diffusing wave spectroscopy (Maret, 1997) is a technique to investigate dynamical processes of the medium by measuring the time autocorrelation function of the

intensity of multiply scattered light. This technique probes, for example, the motion of scatterers on time scales much smaller than in quasielastic light scattering. It requires a good understanding of multiple light scattering and has been applied to all sorts of soft matter such as colloids, foams, emulsions, and recently nematic liquid crystals (Maret, 1997).

Several open problems exist that have so far received little attention. First, it was shown that multiple scattering in an aligned nematic tends to equipartition the energy of extraordinary and ordinary waves in a rather nontrivial way, but independent of the precise selection rules in scattering. The equipartition law was predicted first for multiple scattering of elastic waves (Weaver, 1982), which also possess two independent modes of propagation. An experimental verification of this law would not only be direct evidence for the diffusion approximation, it would also confirm a very specific feature of radiative transfer involving two independent modes that mix by scattering. Such a measurement must involve a detection of energy density rather than one of specific intensity, as is common in optical experiments.

Second, coherent backscattering experiments have already been undertaken in monodomain nematic liquid crystals (Vithana, Asfaw, and Johnson, 1993), following earlier experiments in much stronger scattering nonoriented liquid crystals (Vlasov *et al.*, 1988). This phenomenon involves an interference effect in multiple scattering that is intimately related to reciprocity (van Tiggelen and Maynard, 1997). In principle, coherent backscattering experiments should reveal the anisotropy in diffusion, but the large mean free path (1 mm) of the light has made this feature so far impossible to observe. Coherent backscattering in oriented nematics has been considered numerically (Heiderich, Maynard, and van Tiggelen, 1997). A complete analytical treatment of this effect in nematic liquid crystals has never been undertaken, and only exists for anisotropic scatterers (Kuz'min, Romanov, and Zubkov, 1996) and for anisotropic light propagation in magnetic fields (van Tiggelen, Maynard, and Nieuwenhuizen, 1996). An analytic treatment should reveal how the angular anisotropy of the line shape in coherent backscattering is affected by the optical anisotropy of the nematic, which enters in both the diffusion anisotropy and the boundary conditions. In isotropic media, the angular width of coherent backscattering is given by $\Delta\theta \approx 1/kl^*$, with l^* the transport mean free path and k the wave number. In aligned nematics one could speculate that for each given orientation of the optical axis, two lengths exist that replace the transport mean free path l^* in the backscattering cone of an isotropic system, that is, one for each diagonal polarization channel EE and OO . No coherent backscattering is expected in the crossed-channel EO because different modes have different group velocities (Vithana, Asfaw, and Johnson, 1993).

Finally, diffusing wave spectroscopy shows great promise for the study of nematic liquid crystals. Down to the experimental resolution of 4×10^{-8} s, no deviation of the director dynamics from the Leslie-Erickson

theory has been observed (Kao *et al.*, 1997). It would be interesting to study systems with higher viscosities like polymer liquid crystals and to look for a deviation from hydrodynamic theory. Such deviations, which have been observed in colloidal suspensions (Weitz *et al.*, 1989; Kao *et al.*, 1993), could provide precious information on the statistical physics that governs director fluctuations.

Future research on radiative transfer will also concentrate on more strongly scattering anisotropic materials, for which the approach in this review is relevant. A wealth of materials exist that scatter light strongly and anisotropically, such as porous media filled with nematics (Bellini and Clark, 1996), polymer dispersed liquid crystals (Doane *et al.*, 1986; Drzaic, 1995), focal conic textures in cholesterics (Yang, Chien, and Fung, 1996), and the Blue Phase III (Kutnjak *et al.*, 1995; Lubensky and Stark, 1996; Singh *et al.*, 1997; Englart *et al.*, 1998). The last two materials are especially appealing because they are chiral and possess an intrinsic periodic structure from which light is scattered. The scattering cross section heavily depends on the circular polarization of light. It was found recently that the Blue Phase III constitutes an isotropic phase with strong chiral fluctuations.

Polymer dispersed liquid crystals (PDLC's) have rather dramatic light-scattering properties, which can be switched from an opaque to a clear state by an externally applied electric field. Scattering from PDLC films has been investigated mostly in the anomalous diffraction and Rayleigh-Gans approximation (Žumer and Doane, 1986; Kelly and Palffy-Muhoray, 1994; Drzaic, 1995; Cox *et al.*, 1998). A complete understanding of this transition can only be obtained from the equation of radiative transfer, which covers the whole regime from single to multiple scattering. Applications to lyotropic and polymeric liquid crystals and to liquid crystalline colloids could also be of interest. Filled nematics are nematic liquid crystals doped with isotropic scatterers (Kreuzer, Tschudi, and Eidenschink, 1992). In an ideal situation, i.e., particles dispersed in a uniformly aligned nematic, the only source of anisotropic light diffusion is the host medium, and not scattering from director fluctuations, which is negligible compared to the scattering from particles. However, a clear experiment requires the director field around the particles to be undistorted, in order to exclude light scattering from the nonuniform director field. This might be achieved by weak anchoring of the director at the surface of the particle and by applying a magnetic field.

ACKNOWLEDGMENTS

We have benefited from long-term collaborations, discussions, and exchange of ideas, including unpublished results, with a large number of people who have posed pertinent questions. We would like to thank (in alphabetical order) M. Copič, A. Heiderich, K. A. Jester, M. H. Kao, T. Lubensky, G. Maret, R. Maynard, A. Mertelj, P. Palffy-Muhoray, J. Prost, Ch. Vanneste, D. A. Weitz, D. S. Wiersma, and A. Yodh.

REFERENCES

- Akkermans, E., G. Montambaux, J.-L. Pichard, and J. Zinn-Justin, 1995, Eds., *Mesoscopic Quantum Physics* (Elsevier, Amsterdam).
- Akkermans, E., P. E. Wolf, and R. Maynard, 1986, *Phys. Rev. Lett.* **56**, 1471.
- Ashcroft, N. W., and N. D. Mermin, 1976, *Solid State Physics* (Saunders, Fort Worth, TX), Chap. 8.
- Barabanenkov, Yu. N., and V. D. Ozrin, 1991, *Phys. Lett. A* **154**, 38.
- Barabanenkov, Yu. N., and V. D. Ozrin, 1995, *Phys. Lett. A* **206**, 116.
- Barabanenkov, Yu. N., L. M. Zurk, and M. Yu. Barabanenkov, 1995, *J. Electromagn. Waves Appl.* **9**, 1393.
- Beenakker, C. W. J., 1997, *Rev. Mod. Phys.* **69**, 731.
- Bellini, T., and N. A. Clark, 1996, in *Liquid Crystals in Complex Geometries*, edited by G. P. Crawford and S. Žumer (Taylor & Francis, London), Chap. 19, p. 381.
- Bellini, T., N. A. Clark, V. Gegiorgio, F. Mantegazza, and G. Natale, 1998, *Phys. Rev. E* **57**, 2996.
- Berkovits, R., and S. Feng, 1994, *Phys. Rep.* **238**, 135.
- Berne, P. J., and R. Pecora, 1976, *Dynamic Light Scattering, with Applications to Chemistry, Biology and Physics* (Wiley, New York).
- Boas, D. A., L. J. Campell, and A. G. Yodh, 1995, *Phys. Rev. Lett.* **75**, 1855.
- Boas, D. A., M. A. O'Leary, B. Chance, and A. Yodh, 1994, *Proc. Natl. Acad. Sci. USA* **91**, 4887.
- Boots, H. M. J., 1994, *J. Opt. Soc. Am. A* **11**, 2539.
- Born, M., and E. Wolf, 1975, *Principles of Optics* (Pergamon, Oxford).
- Browsers, R., and T. Deeming, 1984, *Astrophysics* (Jones and Bartlett, Boston).
- Campillo, M., L. Margerin, and N. Shapiro, 1999, in *Wave Diffusion in Complex Media*, edited by J. P. Fouque (Kluwer, Dordrecht), pp. 383–404.
- Chaikin, P. M., and T. C. Lubensky, 1995, *Principles of Condensed Matter Physics* (Cambridge University Press, Cambridge/New York).
- Chance, B., 1989, *Photon Migration in Tissues* (Plenum, New York).
- Chandrasekhar, S., 1960, *Radiative Transfer* (Dover, New York).
- Chandrasekhar, S., 1977, *Liquid Crystals* (Cambridge University Press, Cambridge).
- Collings, P., 1997, private communication.
- Cox, S. J., V. Yu. Reshetnyak, and T. J. Sluckin, 1998, *J. Phys. D* **31**, 1611.
- de Boer, J. F., M. P. van Albada, and A. Lagendijk, 1990, *Phys. Rev. Lett.* **64**, 2787.
- de Gennes, P. G., and J. Prost, 1993, *The Physics of Liquid Crystals*, 2nd edition (Clarendon, Oxford).
- de Haan, J. F., P. B. Bosma, and J. W. Hovenier, 1987, *Astron. Astrophys.* **183**, 371.
- de Jeu, W. H., 1980, *Physical Properties of Liquid Crystalline Materials* (Gordon and Breach, New York).
- Derode, A., Ph. Roux, and M. Fink, 1995, *Phys. Rev. Lett.* **75**, 4206.
- Doane, J. W., N. A. Vaz, B. G. Wu, and S. Žumer, 1986, *Appl. Phys. Lett.* **48**, 269.
- Drzaic, P. S., 1995, *Liquid Crystal Dispersions* (World Scientific, Singapore).
- Durian, D. J., D. A. Weitz, and D. J. Pine, 1991, *Science* **252**, 686.
- Englert, J., L. Longa, H. Stark, and H.-R. Trebin, 1998, *Phys. Rev. Lett.* **81**, 1457.
- Erbacher, F., R. Lenke, and G. Maret, 1993, *Europhys. Lett.* **21**, 551.
- Forster, D., 1975, *Hydrodynamic Fluctuations, Broken Symmetry and Correlation Functions*, *Frontiers in Physics*, edited by D. Pines (Benjamin, Reading, MA).
- Forster, D., T. Lubensky, P. Martin, J. Swift, and P. Pershan, 1971, *Phys. Rev. Lett.* **26**, 1016.
- Frisch, U., 1968, in *Probabilistic Methods in Applied Mathematics*, edited by A. T. Bharucha-Reid (Academic, New York), Vol. 1, pp. 75–198.
- Furst, E. M., and A. P. Gast, 1998, *Phys. Rev. E* **58**, 3372.
- Gang, H., A. H. Krall, and D. A. Weitz, 1994, *Phys. Rev. Lett.* **73**, 3435.
- Genack, A. Z., 1990, in *Scattering and Localization of Classical Waves in Random Media*, edited by Ping Sheng (World Scientific, Singapore), pp. 207–311.
- Genack, A. Z., and N. Garcia, 1993, *Europhys. Lett.* **21**, 753.
- Gisler, T., and D. A. Weitz, 1999, *Phys. Rev. Lett.* **82**, 1606.
- Grabert, H., 1982, *Projection Operator Techniques in Nonequilibrium Statistical Mechanics* (Springer-Verlag, Berlin).
- Heckmeier, M., S. E. Skipetrov, G. Maret, and R. Maynard, 1997, *J. Opt. Soc. Am. A* **14**, 185.
- Heiderich, A., R. Maynard, and B. A. van Tiggelen, 1997, *J. Phys. II* **7**, 765.
- Höhler, R., S. Cohen-Addad, and H. Hoballah, 1997, *Phys. Rev. Lett.* **79**, 1154.
- Holstein, T., 1947, *Phys. Rev.* **72**, 1212.
- Ishimaru, A., 1978, *Wave Propagation in Random Media*, Vols. 1 and 2 (Academic, New York).
- John, S., 1991, *Phys. Today* **44** (5), 32.
- Kao, M. H., K. A. Jester, A. G. Yodh, and P. J. Collins, 1997, *Phys. Rev. Lett.* **77**, 639.
- Kao, M. H., A. G. Yodh, and D. J. Pine, 1993, *Phys. Rev. Lett.* **70**, 242.
- Kelly, J. R., and P. Palfy-Muhoray, 1994, *Mol. Cryst. Liq. Cryst.* **243**, 11.
- Kreuzer, M., T. Tschudi, and R. Eidenschink, 1992, *Mol. Cryst. Liq. Cryst.* **223**, 219.
- Kuga, Y., and A. Ishimaru, 1984, *J. Opt. Soc. Am. A* **1**, 831.
- Kutnjak, Z., C. W. Garland, J. L. Passmore, and P. J. Collings, 1995, *Phys. Rev. Lett.* **74**, 4859.
- Kuz'min, V. L., V. P. Romanov, and L. A. Zubkov, 1994, *Phys. Rep.* **248**, 71, Sec. VIII.
- Kuz'min, V. L., V. P. Romanov, and L. A. Zubkov, 1996, *Phys. Rev. E* **54**, 6798.
- Labeyrie, G., J.-C. de Tomasi, J.-C. Bernard, C. A. Müller, Ch. Miniatura, and R. Kaiser, 1999, *Phys. Rev. Lett.* **83**, 5266.
- Lacoste, D., and B. A. van Tiggelen, 1999, *Europhys. Lett.* **45**, 721.
- Lagendijk, A., and B. A. van Tiggelen, 1996, *Phys. Rep.* **270**, 143.
- Landau, L. D., E. M. Lifshitz, and L. P. Pitaevskii, 1984, *Electrodynamics of Continuous Media*, 2nd edition (Pergamon, Oxford).
- Langevin, D., 1974, *Solid State Commun.* **14**, 435.
- Langevin, D., and M.-A. Bouchiat, 1975, *J. Phys. (France)* **C1**, 197.
- Lax, M., and D. F. Nelson, 1971, *Phys. Rev. B* **4**, 3694.

- Li, J. H., A. A. Lisyanski, T. D. Cheung, D. Livdan, and A. Z. Genack, 1993, *Europhys. Lett.* **22**, 675.
- Liu, M., 1994, *Phys. Rev. E* **50**, 2925.
- Lubensky, T. C., and H. Stark, 1996, *Phys. Rev. E* **53**, 714.
- Mahan, G. D., 1981, *Many Particle Physics* (Plenum, New York), Chap. 7.
- Maret, G., 1997, *Curr. Opin. Colloid Interface Sci.* **2**, 251.
- Maret, G., and P. E. Wolf, 1987, *Z. Phys. B: Condens. Matter* **65**, 409.
- Margerin, L., M. Campillo, and B. A. van Tiggelen, 1998, *Geophys. J. Int.* **134**, 596.
- Martinez, A. S., and R. Maynard, 1994, *Phys. Rev. B* **50**, 3714.
- Mertelj, A., and M. Copic, 1997, *Phys. Rev. E* **55**, 504.
- Mihalas, D., 1978, *Stellar Atmospheres*, 2nd edition (Freeman, San Francisco).
- Mishchenko, M. I., L. D. Travis, and J. W. Hovenier, 1999, Eds., *Light Scattering by Nonspherical Particles: Theory, Measurements and Applications* (Academic, San Diego).
- Nehring, J., and A. Saupe, 1971, *J. Chem. Phys.* **54**, 337.
- Orsay Liquid Crystal Group, 1969, *Phys. Rev. Lett.* **22**, 1361.
- Papanicolaou, G. C., and R. Burridge, 1975, *J. Math. Phys.* **16**, 2074.
- Pergamenschik, V. M., 1998, *Phys. Rev. E* **58**, R16.
- Pine, D. J., D. A. Weitz, J. X. Zhu, and E. Herbolzheimer, 1990, *J. Phys. (France)* **18**, 2101.
- POAN Research Group, 1998, *New Aspects of Electromagnetic and Acoustic Wave Diffusion*, edited by J. Kuhn (Springer-Verlag, Heidelberg/New York).
- Pomeau, Y., and P. Résibois, 1975, *Phys. Rep.* **19**, 63.
- Rikken, G. L. J. S., and B. A. van Tiggelen, 1996, *Nature (London)* **381**, 54.
- Romanov, V. P., and A. N. Shalaginov, 1988, *Opt. Spectrosc.* **64**, 774.
- Roux, Ph., and M. Fink, 1995, *Europhys. Lett.* **32**, 25.
- Scheffold, F., and G. Maret, 1998, *Phys. Rev. Lett.* **81**, 5800.
- Schuster, A., 1905, *Astrophys. J.* **21**, 1.
- Shalaginov, A. N., 1994, *Phys. Rev. E* **49**, 2472.
- Sharvin, D. Y., and Y. V. Sharvin, 1981, *JETP Lett.* **34**, 272.
- Sheng, Ping, 1995, *Introduction to Wave Scattering, Localization and Mesoscopic Phenomena* (Academic, San Diego).
- Silverman, M. P., W. Trange, J. Badoz, and I. A. Vitkin, 1999, *Opt. Commun.* (in press).
- Singh, U., P. J. Collings, C. J. Booth, and J. W. Goodby, 1997, *J. Phys. II* **7**, 1683.
- Sobolev, V. V., 1963, *A Treatise on Radiative Transfer* (Van Nostrand, Princeton).
- Sobolev, V. V., 1975, *Light Scattering in Planetary Atmospheres* (Pergamon, New York).
- Sparenberg, A., G. L. J. A. Rikken, and B. A. van Tiggelen, 1997, *Phys. Rev. Lett.* **79**, 757.
- Stark, H., 1998, *Mol. Cryst. Liq. Cryst.* **321**, 403.
- Stark, H., M. H. Kao, K. A. Jester, T. C. Lubensky, and A. G. Yodh, 1997, *J. Opt. Soc. Am. A* **14**, 156.
- Stark, H., and T. C. Lubensky, 1996, *Phys. Rev. Lett.* **77**, 2229.
- Stark, H., and T. C. Lubensky, 1997, *Phys. Rev. E* **55**, 514.
- Stephen, M. J., and J. P. Straley, 1974, *Rev. Mod. Phys.* **46**, 617.
- Val'kov, Yu. A., and V. P. Romanov, 1986, *Sov. Phys. JETP* **63**, 737.
- van Albada, M. P., and A. Lagendijk, 1985, *Phys. Rev. Lett.* **55**, 2692.
- van Albada, M. P., and A. Lagendijk, 1987, *Phys. Rev. B* **36**, 2353.
- van de Hulst, H. C., 1980, *Multiple Light Scattering*, Vols. I & II (Academic, New York).
- van Rossum, M. C. W., and Th. M. Nieuwenhuizen, 1999, *Rev. Mod. Phys.* **71**, 313.
- van Tiggelen, B. A., 1999, in *Diffuse Waves in Complex Media*, edited by J. P. Fouque (Kluwer, Dordrecht), p. 1.
- van Tiggelen, B. A., A. Heiderich, and R. Maynard, 1997, *Mol. Cryst. Liq. Cryst.* **293**, 205.
- van Tiggelen, B. A., and A. Lagendijk, 1993, *Europhys. Lett.* **23**, 311.
- van Tiggelen, B. A., and R. Maynard, 1997, in *Wave Propagation in Complex Media*, edited by G. Papanicolaou (Springer-Verlag, New York), p. 247.
- van Tiggelen, B. A., R. Maynard, and A. Heiderich, 1996, *Phys. Rev. Lett.* **77**, 639.
- van Tiggelen, B. A., R. Maynard, and Th. M. Nieuwenhuizen, 1996, *Phys. Rev. E* **53**, 2881.
- Vertogen, G., and W. H. de Jeu, 1988, *Thermotropic Liquid Crystals, Fundamentals* (Springer, Berlin).
- Virmont, J., and G. Ledanois, 1998, in *New Aspects of Electromagnetic and Acoustic Wave Diffusion*, edited by POAN Research Group (Springer, Heidelberg), p. 35.
- Vithana, H. K. M., L. Asfaw, and D. L. Johnson, 1993, *Phys. Rev. Lett.* **70**, 3561.
- Vlasov, D. V., L. A. Zubkov, N. V. Orekhova, and V. P. Romanov, 1988, *Pis'ma Zh. Eksp. Teor. Fiz. [JETP Lett.]* **48**, 86.
- Wiersma, D. S., P. Bartolini, A. Lagendijk, and R. Righini, 1997, *Nature (London)* **390**, 671.
- Wiersma, D. S., A. Muzzi, M. Colocci, and R. Righini, 1999, *Phys. Rev. Lett.* **83**, 4321.
- Wolf, P. E., and G. Maret, 1985, *Phys. Rev. Lett.* **55**, 2696.
- Weaver, R. L., 1982, *J. Acoust. Soc. Am.* **71**, 1608.
- Weitz, D. A., and D. J. Pine, 1992, in *Dynamic Light Scattering*, edited by W. Brown (Oxford University, New York), p. 652.
- Weitz, D. A., D. J. Pine, P. N. Pusey, and R. J. A. Tough, 1989, *Phys. Rev. Lett.* **63**, 1747.
- Yang, D.-K., L.-C. Chien, and Y. K. Fung, 1996, in *Liquid Crystals in Complex Geometries*, edited by G. P. Crawford and S. Zumer (Taylor & Francis, London), Chap. 5, p. 103.
- Yodh, A. G., and B. Chance, 1995, *Phys. Today* **48** (3), 34.
- Zumer, S., and J. W. Doane, 1986, *Phys. Rev. A* **34**, 3373.